

# Total, quantum, and classical measures of antcoherence for mixed spin states

Jérôme Denis,<sup>1,2,\*</sup> Tara Lacaille,<sup>2</sup> John Martin,<sup>2,†</sup> and Eduardo Serrano-Ensástiga<sup>2,‡</sup>

<sup>1</sup>*Institute of Quantum Precision Measurement, State Key Laboratory of Radio Frequency Heterogeneous Integration, College of Physics and Optoelectronic Engineering, Shenzhen University, Shenzhen 518060, China*

<sup>2</sup>*Institut de Physique Nucléaire, Atomique et de Spectroscopie, CESAM, University of Liège B-4000 Liège, Belgium*

(Dated: May 27, 2026)

Anticoherent spin states have isotropic low-order spin moments and are relevant to direction-independent metrology and quantum reference-frame alignment. In contrast to pure states, for mixed states such isotropy may originate either from genuine quantum correlations or from classical statistical mixing. We introduce an axiomatic framework for mixed-state  $t$ -anticoherence based on the symmetric qubit embedding. We distinguish *total*  $t$ -anticoherence, non-decreasing under  $SU(2)$ -covariant channels, from *quantum*  $t$ -anticoherence, defined as a resource monotone relative to a chosen total measure and constrained to coincide with it on pure states. This yields a *classical* contribution as their difference. We construct total measures based on reduced-state purity, Hilbert–Schmidt distance, and cumulative multipoles, and we discuss fidelity-based total candidates. We construct quantum counterparts via convex-roof extensions of pure-state functionals tied to bipartite entanglement in the symmetric sector. We provide explicit mixed-state examples, identify states with maximal quantum anticoherence supported on anticoherent subspaces, study robustness under particle loss for different types of states, and characterize the trade-off between purity and the maximal achievable anticoherence order.

## I. INTRODUCTION

Spin states that lack any apparent spatial orientation, due to quantum superpositions, play an important role in quantum information, quantum metrology, and the theory of quantum reference frames. Such states are particularly relevant whenever no shared spatial reference frame is available, or when one seeks to suppress or average out directional information. This notion is captured by the concept of *anticoherent* (AC) spin states, originally introduced for pure states as those whose low-order spin moments are isotropic [1]. In particular, anticoherence can be viewed as the opposite of spin coherence: whereas coherent spin states are “most classical” in that they point maximally along some direction, AC states suppress directional moments (e.g.  $\langle \mathbf{J} \rangle = 0$  at first order) by suitable quantum superpositions. AC states exhibit remarkable properties, ranging from connections to spherical designs and Majorana constellations to entanglement classification, robust geometric phases and optimal sensitivity bounds in direction-independent metrology [2–17].

From an operational perspective, the isotropy of a spin state determines its usefulness as a quantum reference frame. States that break rotational symmetry can serve as tokens for spatial orientation and enable reference-frame alignment [18–24], while isotropic states are useless for this task. This viewpoint is formalized within the resource theory of  $SU(2)$  asymmetry, where asymmetry with respect to rotations quantifies the ability of a

quantum system to encode and transmit directional information [25–28]. In this framework,  $SU(2)$ -covariant operations represent free operations that cannot increase directional information. A fundamental example is provided by random global rotations, which model the absence of a shared reference frame or deliberate averaging over orientations [25]. AC states, therefore, correspond to highly symmetric states within this resource theory, carrying no orientation information up to a given order.

Beyond their conceptual role, pure-state anticoherence has found concrete applications in several operational settings. In quantum metrology, highly AC states display optimal or near-optimal performance in fidelity-based estimation tasks that do not assume any preferred spatial direction, reflecting their uniform sensitivity to rotations and their close connection to spherical designs [4, 11, 16, 29]. More generally, AC states have been identified as optimal quantum rotosensors and as enabling multiparameter estimation of rotational ( $SO(3)$ ) parameters (e.g. Euler angles) in suitable setups [8–11]. For mixed states, for instance in noisy rotational metrology, mixtures of AC states are also suitable for rotational metrological scenarios [29].

Anticoherence has also been investigated as a marker of *extreme quantumness*: maximally AC states can form orthonormal bases whose elements exhibit strong multipartite entanglement and pronounced nonclassical behavior [2]. Closely related ideas appear in reference-frame alignment protocols: states with strong low-order directional moments can serve as tokens of an absolute direction, whereas anticoherent states suppress such directional bias and are instead well suited to isotropic estimation of rotations or frame misalignment [8]. These results motivate the experimental realization of anticoherent states [12, 30, 31] and similar states such as ran-

\* jdenis@szu.edu.cn

† jmartin@uliege.be

‡ ed.ensastiga@uliege.be

dom and  $t$ -design states [32, 33].

While the theory of anticonherence for pure states is now well established, a systematic extension to mixed states is still lacking. For mixed states, isotropy of low-order moments may arise either from genuinely quantum correlations or from classical statistical mixing, such as averaging over unknown orientations. As a consequence, a single scalar quantity is generally insufficient to capture the physical content of anticonherence in the mixed-state regime, particularly from the viewpoint of quantum resources and asymmetry. This tension is already visible in existing quantifiers: several anticonherence measures have been proposed to quantify isotropy for arbitrary states [34], including distance-based constructions. Yet even the maximally mixed state (MMS), arguably the most classical mixed state, appears maximally anticonherent in the sense of low-order isotropy.

In this work, we introduce an axiomatic framework for *mixed-state*  $t$ -anticonherence that makes this distinction explicit. We identify two complementary notions: (i) *total*  $t$ -anticonherence, which quantifies the isotropy of order  $t$  irrespective of its classical or quantum origin, and (ii) *quantum*  $t$ -anticonherence, which isolates the intrinsically quantum contribution and behaves as a quantum resource monotone. Operationally, total  $t$ -anticonherence characterizes the inability of a state to function as a reference frame at resolution  $t$ , while quantum  $t$ -anticonherence captures the part of this isotropy that cannot be generated by classical mixing. From a resource-theoretic perspective, this decomposition could also be interpreted as separating the classical and quantum resources required to prepare such states.

These two notions are naturally associated with distinct operational frameworks. Total  $t$ -anticonherence is closely related to the resource theory of  $SU(2)$  asymmetry and to reference-frame alignment tasks, where random rotations represent free noise. Quantum  $t$ -anticonherence, on the other hand, is tied to entanglement properties in the symmetric-qubit embedding [6, 7, 35–37] and quantifies isotropy arising from genuinely quantum correlations. This separation allows one to define a meaningful classical contribution to isotropy as the difference between total and quantum  $t$ -anticonherence.

We formulate axioms for both types of measures, construct explicit examples based on distances to the MMS state and on convex-roof extensions, and show that the total contribution always upper bounds the quantum contribution. Finally, we clarify the relation between our framework and existing tensor-based descriptions of angular structure, in particular the cumulative multipole measures defined and studied in [3, 38, 39].

The paper is organized as follows. Section II introduces mixed-state  $t$ -anticonherence and the axiomatic framework for total, quantum, and classical measures. Section III presents explicit constructions of these measures and their properties, including distance-based and cumulative-multipole formulations. Section IV provides explicit evaluations, and Section V discusses applications

to representative mixed states, robustness under particle loss, and the trade-off between purity and the maximal achievable anticonherence order. We conclude in Sec. VI with some final comments.

## II. AXIOMATIC FRAMEWORK FOR MIXED-STATE ANTICOHERENCE MEASURES

### A. Mixed-state $t$ -anticonherence

Let  $\mathcal{H}_j$  denote the Hilbert space of a spin- $j$  system, with standard angular-momentum basis  $\{|j, m\rangle\}_{m=-j}^j$  (eigenstates of  $J^2$  and  $J_z$ ). Using the standard identification between  $\mathcal{H}_j$  and the fully symmetric subspace of  $N = 2j$  qubits, any state  $\rho \in \mathcal{D}(\mathcal{H}_j)$  defines a symmetric  $N$ -qubit state  $\rho_S$ . For  $t \in \{1, \dots, N\}$  we denote by

$$\rho_t = \text{Tr}_{N-t}(\rho_S) \quad (1)$$

the reduced state on  $t$  qubits, supported on the symmetric subspace of dimension  $t + 1$ .

It is often convenient to characterize spin states in terms of irreducible tensor operators  $\{T_{LM}\}$  [40]<sup>1</sup>. Any spin- $j$  state  $\rho$  can be expanded as

$$\rho = \frac{\mathbb{1}}{2j+1} + \sum_{L=1}^{2j} \sum_{M=-L}^L \rho_{LM} T_{LM}. \quad (2)$$

The coefficients  $\rho_{LM}$  are the multipole moments of  $\rho$  and encode its angular structure at rank  $L$ .

**Definition 1.** A spin state  $\rho$ , pure or mixed, is *t-anticonherent* (*t-AC*) if all its multipole moments up to rank  $t$  vanish, namely

$$\rho_{LM} = 0, \quad 1 \leq L \leq t, \quad -L \leq M \leq L. \quad (3)$$

Equivalently, all spin moments up to order  $t$  are isotropic.

Using the standard identification between  $\mathcal{H}_j$  and the fully symmetric subspace of  $N = 2j$  qubits, this definition admits an equivalent reduced-state formulation. If  $\rho_S$  denotes the corresponding symmetric  $N$ -qubit state and

$$\rho_t = \text{Tr}_{N-t}(\rho_S) \quad (4)$$

is its reduced state on  $t$  qubits, then

$$\rho \text{ is } t\text{-AC} \quad \Leftrightarrow \quad \rho_t = \frac{\mathbb{1}_{t+1}}{t+1}. \quad (5)$$

Indeed, the partial trace map in the irreducible tensor basis reads [41]

$$\rho_t = \sum_{L=0}^t \sum_{M=-L}^L \frac{t!}{N!} \sqrt{\frac{(N-L)!(N+L+1)!}{(t-L)!(t+L+1)!}} \rho_{LM} T_{LM}^{(t)}, \quad (6)$$

<sup>1</sup> With the Hilbert-Schmidt normalization  $\text{Tr}(T_{LM}^\dagger T_{L'M'}) = \delta_{LL'} \delta_{MM'}$ .

where  $T_{LM}^{(t)}$  denotes the irreducible tensor operator acting on the spin- $t/2$  Hilbert space. Thus  $\rho_t$  depends only on the coefficients  $\rho_{LM}$  with  $L \leq t$ , while all higher-rank components vanish under reduction. Consequently,  $\rho_t$  is maximally mixed if and only if all multipole moments of  $\rho$  up to rank  $t$  vanish.

Let us note two immediate consequences of Definition 1. First,  $t$ -anticoherence is monotone in the order: if  $\rho$  is  $t$ -AC, then it is  $t'$ -AC for every  $t' \leq t$ . This follows either from the nesting of partial traces,  $\rho_{t'} = \text{Tr}_{t-t'}(\rho_t)$ , together with  $\rho_t = \mathbb{1}_{t+1}/(t+1)$ , or equivalently from (6), since vanishing multipoles up to rank  $t$  implies vanishing multipoles up to rank  $t'$ . Second,  $t$ -anticoherence is stable under particle loss: for any  $q > t$ , if  $\rho_q = \text{Tr}_{N-q}(\rho_S)$ , then  $(\rho_q)_t = \text{Tr}_{q-t}(\rho_q) = \text{Tr}_{N-t}(\rho_S) = \rho_t$  by the associativity of the partial trace, so  $\rho_t = \mathbb{1}_{t+1}/(t+1)$  implies  $(\rho_q)_t = \mathbb{1}_{t+1}/(t+1)$ , i.e.,  $\rho_q$  is again  $t$ -AC.

Definition 1 reduces to the standard notion of  $t$ -anticoherence for pure states [42] given by Zimba [1]. For mixed states, however, isotropy up to order  $t$  can arise either from classical statistical mixing, genuine quantum correlations, or both; this motivates the distinction introduced in this work between total, quantum, and classical measures of anticoherence.

## B. Total $t$ -AC measure

A measure of total  $t$ -AC quantifies the isotropy, or lack of directional information, of order  $t$  independently of its classical or quantum origin<sup>2</sup>.

**Definition 2.** A function  $\mathcal{A}_t^T : \mathcal{D}(\mathcal{H}_j) \rightarrow [0, 1]$  is a total  $t$ -AC measure if it satisfies:

- (T1)  $\mathcal{A}_t^T(\rho) = 1$  iff  $\rho$  is  $t$ -AC;
- (T2)  $\mathcal{A}_t^T(\rho) = 0$  iff  $\rho$  is pure and coherent;
- (T3)  $\mathcal{A}_t^T(U\rho U^\dagger) = \mathcal{A}_t^T(\rho)$  for all  $U \in \text{SU}(2)$ ;
- (T4) *Monotonicity under SU(2)-covariant noise:* For every SU(2)-covariant channel  $\Phi : \mathcal{D}(\mathcal{H}_j) \rightarrow \mathcal{D}(\mathcal{H}_j)$ , i.e. every completely positive trace-preserving map such that

$$\Phi(U\rho U^\dagger) = U\Phi(\rho)U^\dagger \quad (7)$$

for all  $U \in \text{SU}(2)$  and  $\rho \in \mathcal{D}(\mathcal{H}_j)$ , one has

$$\mathcal{A}_t^T(\Phi(\rho)) \geq \mathcal{A}_t^T(\rho) \quad (8)$$

for all  $\rho \in \mathcal{D}(\mathcal{H}_j)$ .

Axioms (T3)–(T4) place total  $t$ -AC in direct correspondence with the resource-theoretic notion of SU(2)-*asymmetry* (or, equivalently, the ability to encode directional information) [25–27, 43, 44]. In this framework, *free operations* are precisely the SU(2)-covariant channels  $\Phi$ , while *free states* are the SU(2)-invariant states. Since we work on a fixed spin- $j$  irreducible representation, Schur's lemma implies that the unique free state is the MMS state  $\rho_0 \equiv \mathbb{1}_{2j+1}/(2j+1)$ . Axiom (T4) expresses that total  $t$ -anticoherence cannot decrease under free SU(2) noise that degrades directional information. Operationally, a large value of  $\mathcal{A}_t^T(\rho)$  means that  $\rho$  is a poor indicator for the alignment of the reference frame at resolution  $t$ , as its low-order multipole moments are suppressed.

The next lemma presents a basic structural property of SU(2)-covariant channels on a fixed spin sector, which will be used repeatedly in the construction of explicit total measures.

**Lemma 1** ([45]). *Let  $\Phi$  be an SU(2)-covariant channel on  $\mathcal{H}_j$ . Then  $\Phi$  is unital, i.e.,  $\Phi(\mathbb{1}) = \mathbb{1}$ , and in particular the MMS state  $\rho_0$  is a fixed point of  $\Phi$ .*

Lemma 1 explains why the isotropic MMS state will naturally play the role of reference point in the distance- and purity-based construction of AC measures: any SU(2)-covariant channel fixes it.

Random global rotations with a conjugation-invariant probability density,

$$\rho \mapsto \int_{\text{SU}(2)} p(U) U\rho U^\dagger dU, \quad p(VUV^\dagger) = p(U), \quad (9)$$

form a natural subclass of SU(2)-covariant channels and describe *classical* uncertainty about the laboratory orientation. They model the absence of a shared reference frame or deliberate orientation averaging [25]. However, the complete set of SU(2)-covariant channels is strictly larger: it contains all CPTP maps that commute with the rotation action, including irreversible dissipative processes [41, 46, 47] and measure-and-reprepare (entanglement-breaking) operations, provided they remain *direction insensitive*.

Since the operator space on a fixed spin- $j$  irrep decomposes multiplicity-free into irreducible tensor sectors, covariance implies, by Schur's lemma, that  $\Phi$  acts diagonally on irreducible tensor operators,

$$\Phi(T_{LM}) = f_L T_{LM} \quad \forall L, M, \quad (10)$$

with  $f_L$  real numbers such that  $|f_L| \leq 1$ ; in particular, one always has  $f_0 = 1$  (trace preservation), and complete positivity imposes nontrivial constraints on the admissible values of  $(f_1, \dots, f_{2j})$ , see [48, 49]<sup>3</sup>. Therefore, from

<sup>2</sup> The definition (1) of  $t$ -anticoherence is valid for all  $t \in \{1, \dots, N\}$ . Whenever we consider pure states, we usually assume  $t \leq N/2$ .

<sup>3</sup> For random global rotations of the form (9) with  $p$  depending

the expansion (2), one has

$$\Phi(\rho) = \frac{\mathbb{1}}{2j+1} + \sum_{L=1}^{2j} \sum_{M=-L}^L f_L \rho_{LM} T_{LM}. \quad (12)$$

Thus, a covariant channel may attenuate each multipole rank  $L$  by an independent factor  $f_L$  while treating all components  $M$  identically.

### C. Quantum $t$ -anticoherence measure

While total  $t$ -anticoherence quantifies isotropy independently of its origin, it is useful to single out the contribution stemming from genuinely quantum correlations. For mixed states, this leads to the notion of *quantum  $t$ -anticoherence measures*, which must behave as resource monotones and remain non-increasing under probabilistic state preparation.

Given a total  $t$ -anticoherence measure  $\mathcal{A}_t^T$  according to Definition 2, we define a corresponding notion of quantum  $t$ -anticoherence as follows.

**Definition 3.** A function  $\mathcal{A}_t^Q : \mathcal{D}(\mathcal{H}_j) \rightarrow [0, 1]$  is called a quantum  $t$ -anticoherence measure associated with  $\mathcal{A}_t^T$  if it satisfies:

(Q1) Vanishing on separable states:  $\mathcal{A}_t^Q(\rho) = 0$  for every  $\rho$  corresponding to a fully separable multiqubit symmetric state  $\rho_S^4$ .

(Q2) Pure-state consistency with the chosen total measure<sup>5</sup>: for all pure states  $|\psi\rangle$ ,

$$\mathcal{A}_t^Q(|\psi\rangle\langle\psi|) = \mathcal{A}_t^T(|\psi\rangle\langle\psi|). \quad (14)$$

(Q3) SU(2) invariance:  $\forall U \in \text{SU}(2)$

$$\mathcal{A}_t^Q(U\rho U^\dagger) = \mathcal{A}_t^Q(\rho). \quad (15)$$

---

only on the rotation angle, the coefficients  $f_L$  are the angular averages of the corresponding irreducible characters,

$$f_L = \frac{1}{2L+1} \int_{\text{SU}(2)} p(U) \chi^{(L)}(U) dU, \quad (11)$$

where  $\chi^{(L)}$  is the character of the spin- $L$  representation. In particular,  $f_0 = 1$  (trace preservation), and for  $L \geq 1$  the values  $f_L$  quantify how strongly the random rotations damp the rank- $L$  tensor components.

<sup>4</sup> Equivalently,  $\mathcal{A}_t^Q(\rho) = 0$  for every symmetric state that is separable across the bipartition  $t|N-t$ , since in the symmetric subspace bipartite separability implies full separability. Such symmetric states are of the form

$$\rho_S = \int d\mu(|n\rangle) P(n) (|n\rangle\langle n|)^{\otimes N} \quad (13)$$

with  $P(n)$  a non-negative function.

<sup>5</sup> In particular, if  $\mathcal{A}_t^T$  coincides on pure states with a previously introduced pure-state anticoherence measure  $\mathcal{A}_t$  in [34], then  $\mathcal{A}_t^Q$  coincides with  $\mathcal{A}_t$  on pure states as well.

(Q4) Convexity:  $\mathcal{A}_t^Q(\sum_i p_i \rho_i) \leq \sum_i p_i \mathcal{A}_t^Q(\rho_i)$ .

(Q5) Average monotonicity under symmetric-sector LOCC: For any state  $\rho$  and every LOCC protocol across the bipartition  $t|N-t$  in the symmetric  $N$ -qubit embedding, whose normalized outcomes remain supported on the symmetric subspace,

$$\mathcal{A}_t^Q(\rho) \geq \sum_k p_k \mathcal{A}_t^Q(\rho_k), \quad (16)$$

where  $\rho_k$  is the corresponding spin-state representatives, obtained with probabilities  $p_k$ .

(Q6) Ordering:  $\forall \rho \in \mathcal{D}(\mathcal{H}_j)$

$$\mathcal{A}_t^Q(\rho) \leq \mathcal{A}_t^T(\rho). \quad (17)$$

Because, in the symmetric  $N$ -qubit subspace, separability across any bipartition  $t|N-t$  is equivalent to full separability, the natural free states for a “quantum anticoherence” resource theory are exactly the fully separable symmetric states (and their convex mixtures). Conversely, any symmetric state that is not of this form is necessarily genuinely multipartite entangled [50]. For any  $q \geq t$ , tracing out  $N-q$  particles is an LOCC operation. After identifying the retained state  $\rho_q$  with a symmetric  $q$ -qubit state and considering the induced bipartition  $t|q-t$ , axiom (Q5) implies that the corresponding order- $t$  quantum contribution cannot increase under particle loss. By convexity (Q4) together with SU(2) invariance (Q3), one also finds that the quantum  $t$ -anticoherence is *non-increasing* under random global rotations (9), in contrast with total  $t$ -anticoherence, which is *non-decreasing* under the same class of operations by axiom (T4).

In the spin- $j$  representation, axiom (Q5) refers to operations that become LOCC after identifying the spin- $j$  state with a symmetric  $N = 2j$  qubit state and splitting those constituents into a  $t$ -particle block and its complement. Physically, these are internal block-local manipulations of the collective spin, assisted by classical feed-forward but unable to generate new quantum correlations across that split; hence they should not increase the genuinely quantum contribution to order- $t$  isotropy.

### D. Classical $t$ -anticoherence measure

The distinction between total and quantum  $t$ -AC naturally leads to a third, complementary notion that captures the isotropy arising from classical mixing, which we call classical  $t$ -AC measure.

**Definition 4.** Given a total measure  $\mathcal{A}_t^T$  and its associated quantum measure  $\mathcal{A}_t^Q$ , we define the classical  $t$ -AC measure  $\mathcal{A}_t^C : \mathcal{D}(\mathcal{H}_j) \rightarrow [0, 1]$  by

$$\mathcal{A}_t^C(\rho) \equiv \mathcal{A}_t^T(\rho) - \mathcal{A}_t^Q(\rho). \quad (18)$$

By axiom (Q6),  $\mathcal{A}_t^C(\rho) \geq 0$  for all states, and by the pure-state consistency (Q2), it vanishes identically on pure states. Hence,  $\mathcal{A}_t^C$  quantifies the contribution to isotropy at order  $t$  that can be attributed to classical statistical mixing rather than to intrinsically quantum correlations. Axioms (Q4) and (Q5) ensure that quantum  $t$ -anticoherence cannot be increased by classical mixing or by operations that do not generate quantum correlations. In contrast to total  $t$ -AC, convexity is therefore an essential requirement.

The separation  $\mathcal{A}_t^T = \mathcal{A}_t^Q + \mathcal{A}_t^C$  makes explicit that a state may display large (or even maximal) *total*  $t$ -anticoherence while having no *quantum* contribution, i.e.  $\mathcal{A}_t^Q = 0$  and  $\mathcal{A}_t^C = \mathcal{A}_t^T$ . The most extreme example is the MMS state  $\rho_0$ , which is  $t$ -AC for every  $t$  since all multipole moments vanish, yet contains no quantum correlations and is therefore naturally assigned  $\mathcal{A}_t^Q(\rho_0) = 0$  (hence  $\mathcal{A}_t^C(\rho_0) = 1$ ) for any possible quantum  $t$ -AC measure. A second example is provided by the equal incoherent mixture of two opposite spin-coherent states along a fixed axis,

$$\rho = \frac{1}{2} |j, j\rangle\langle j, j| + \frac{1}{2} |j, -j\rangle\langle j, -j|, \quad (19)$$

which has  $\langle \mathbf{J} \rangle = 0$  (and thus is perfectly isotropic at first order  $t = 1$ ) purely by classical averaging of two antipodal directions. In particular,  $\rho$  has  $\mathcal{A}_1^C(\rho) = \mathcal{A}_1^T(\rho) = 1$  for any 1-AC measure.

### III. CONSTRUCTIONS OF AC MEASURES

#### A. Total AC measures: General constructions

We begin by constructing several measures of total anticoherence.

##### 1. Purity-based construction

A particularly simple example of a total  $t$ -anticoherence measure is obtained from the purity of the reduced symmetric  $t$ -particle state. We define

$$\mathcal{A}_t^{T,P}(\rho) \equiv \frac{t+1}{t} \left(1 - \text{Tr}(\rho_t^2)\right). \quad (20)$$

This expression coincides with the standard purity-based measure of  $t$ -anticoherence  $\mathcal{A}_t^R$  for pure states [34] and provides a direct extension to mixed states.

**Proposition 1** (Proof in Appendix A 1). *The quantity  $\mathcal{A}_t^{T,P}(\rho)$  satisfies axioms (T1)–(T4) and therefore defines a measure of total  $t$ -anticoherence.*

##### 2. Distance-based construction

Distance-based constructions provide another natural class of total  $t$ -anticoherence candidates. Let  $d(\cdot, \cdot)$  be a

unitarily invariant operator distance on the state space of the symmetric  $t$ -qubit sector. We normalize the distance from the MMS state  $\rho_0^{(t)} \equiv \mathbb{1}_{t+1}/(t+1)$ , by its largest possible value,

$$K_t = \max_{\sigma \in \mathcal{D}(\mathcal{H}_{t/2})} d(\sigma, \rho_0^{(t)}). \quad (21)$$

This leads to the normalized distance-based total anticoherence candidate

$$\mathcal{A}_t^{T,d}(\rho) \equiv 1 - \frac{d(\rho_t, \rho_0^{(t)})}{K_t}. \quad (22)$$

With this convention, states whose  $t$ -body reduction equals the MMS state have maximal total  $t$ -anticoherence, while states farthest from the MMS state have minimal value. For the standard distances considered below, whose maximal distance from  $\rho_0^{(t)}$  is attained exactly on pure states, this construction satisfies axioms (T1), (T2), and (T3). If the maximum is attained only when  $\rho_t$  is pure, then, because  $\rho_t$  is a marginal of a symmetric  $N$ -qubit state, this implies that the original state is a pure spin-coherent state. Only (T4) must be proved separately for all  $SU(2)$ -covariant channels.

In particular, for a fixed integer  $p \geq 1$ , we have the distances

$$d_p(\rho, \sigma) = \|\rho - \sigma\|_p, \quad (23)$$

where  $\rho, \sigma \in \mathcal{D}(\mathcal{H}_j)$ , based on the Schatten  $p$ -norm

$$\|A\|_p = \left( \sum_{i=1}^r \lambda_i^p \right)^{1/p}, \quad (24)$$

where  $\lambda_i$  and  $r$  are the singular values and the rank of  $A$ , respectively.

**Proposition 2** (Proof in Appendix A 2). *The quantity  $\mathcal{A}_t^{T,d}(\rho)$  for the distance based on the Schatten 2-norm (associated with the Hilbert-Schmidt distance) satisfies axioms (T1)–(T4) and therefore defines a measure of total  $t$ -anticoherence.*

We also find numerical evidence that axiom (T4) remains valid for the trace-distance case  $p = 1$ ; a proof is left open.

##### 3. Fidelity-based construction

Another construction is obtained from the Uhlmann-Jozsa fidelity between the reduced state  $\rho_t$  and the MMS state  $\rho_0^{(t)} = \mathbb{1}_{t+1}/(t+1)$  on the symmetric  $t$ -qubit subspace:

$$F(\rho_t, \rho_0^{(t)}) \equiv \left( \text{Tr} \sqrt{\sqrt{\rho_t} \rho_0^{(t)} \sqrt{\rho_t}} \right)^2 = \frac{(\text{Tr} \sqrt{\rho_t})^2}{t+1}. \quad (25)$$

We choose an affine rescaling and define

$$\mathcal{A}_t^{T,F}(\rho) \equiv \frac{(t+1)F - 1}{t} = \frac{(\text{Tr} \sqrt{\rho_t})^2 - 1}{t}. \quad (26)$$

Equivalently,

$$\mathcal{A}_t^{T,F}(\rho) = \frac{(t+1) \left[ 1 - \frac{1}{2} D_B(\rho_t, \rho_0^{(t)}) \right]^2 - 1}{t} \quad (27)$$

in terms of the Bures distance

$$D_B(\sigma, \tau) = \sqrt{2(1 - \sqrt{F(\sigma, \tau)})}. \quad (28)$$

The normalization is such that  $\mathcal{A}_t^{T,F} = 1$  for  $t$ -AC states and  $\mathcal{A}_t^{T,F} = 0$  for spin-coherent states. Indeed,  $F(\rho_t, \rho_0^{(t)}) = 1$  iff  $\rho_t = \rho_0^{(t)}$ , whereas the minimum value  $F(\rho_t, \rho_0^{(t)}) = 1/(t+1)$  is reached iff  $\rho_t$  is pure, which in the symmetric setting implies that  $\rho$  is a pure spin-coherent state. The  $SU(2)$  invariance follows from the unitary invariance of the fidelity,  $F(U\rho_t U^\dagger, U\rho_0 U^\dagger) = F(\rho_t, \rho_0)$ , together with  $U\rho_0^{(t)}U^\dagger = \rho_0^{(t)}$ . Thus  $\mathcal{A}_t^{T,F}$  satisfies axioms (T1)–(T3). Concerning axiom (T4), some care is needed. Although a  $SU(2)$ -covariant channel  $\Phi$  on the full spin- $j$  space induces a linear transformation on the reduced state  $\rho_t$ , this induced reduced map is not, in general, a completely positive trace-preserving channel acting on the whole state space  $\mathcal{D}(\mathcal{H}_{t/2})$ . Therefore one cannot simply invoke monotonicity of the Uhlmann fidelity for an induced channel fixing  $\rho_0^{(t)}$ . Numerical evidence suggests that  $\mathcal{A}_t^{T,F}$  is nevertheless non-decreasing under  $SU(2)$ -covariant noise, but we leave a proof of axiom (T4) for future work.

We conclude this section with a general result, which will prove useful later on the relation between the Uhlmann fidelity and entanglement. Consider a quantum state  $|\psi\rangle$  defined on a composite Hilbert space  $\mathcal{H}_{AB}$ . Then, a measure of entanglement of the state  $|\psi\rangle$  on the bipartition  $A|B$  is given by the entanglement negativity [51]

$$\mathcal{N}_A = \sum_{i>j=1}^{d_A} \alpha_i \alpha_j \quad (29)$$

where the  $\alpha_i$  are the Schmidt coefficients of  $|\psi\rangle$  with respect to the split  $A|B$ . From this definition, we have the following result.

**Proposition 3** (Proof in Appendix A3). *For any composite system  $AB$ , a pure state  $|\psi\rangle \in \mathcal{H}_{AB}$  verifies*

$$F(\rho_A, \rho_0) = \frac{1 + 2\mathcal{N}_A(|\psi\rangle)}{d_A}, \quad (30)$$

where  $\rho_A$  is the reduced state defined on  $A$  obtained by tracing out the subsystem  $B$  and  $\rho_0 = \mathbb{1}_A/d_A$  is the MMS state in  $\mathcal{H}_A$ .

This result gives a direct correspondence between the fidelity-based AC measures (26) of a pure state and its entanglement with respect to the bipartition  $t|N-t$ .

## B. Quantum AC measures: general constructions via convex-roof

We now construct quantum  $t$ -AC measures from pure-state functionals by convex-roof extensions.

### 1. Purity-based construction

For pure symmetric states, the quantity  $1 - \text{Tr}(\rho_t^2)$  coincides with the linear entropy of entanglement across the bipartition  $t|N-t$ . This motivates defining a quantum  $t$ -AC measure for mixed states via the convex-roof construction,

$$\mathcal{A}_t^{Q,\mathcal{P}}(\rho) = \min_{\{p_i, |\psi_i\rangle\}} \sum_i p_i \mathcal{A}_t^{\mathcal{P}}(|\psi_i\rangle), \quad (31)$$

where the minimization runs over all pure-state decompositions of  $\rho$ .

**Proposition 4** (Proof in Appendix A4). *The quantity  $\mathcal{A}_t^{Q,\mathcal{P}}(\rho)$  satisfies axioms (Q1)–(Q6) and therefore defines a quantum measure of  $t$ -AC associated with the total purity-based measure  $\mathcal{A}_t^{T,\mathcal{P}}$ .*

**Proposition 5** (Proof in Appendix A5). *For all mixed states  $\rho \in \mathcal{D}(\mathcal{H}_j)$  and all  $t \in \{1, 2, \dots, N-1\}$ ,*

$$\frac{\mathcal{A}_t^{Q,\mathcal{P}}(\rho)}{\mathcal{A}_{N-t}^{Q,\mathcal{P}}(\rho)} = \frac{(t+1)(N-t)}{t(N+1-t)}. \quad (32)$$

### 2. Based on convex distances

We will use a distance  $d$  that is convex in its first argument. That is, for all  $\rho_1, \rho_2, \sigma \in \mathcal{D}(\mathcal{H}_j)$  and all  $\lambda \in [0, 1]$ , it satisfies

$$d(\lambda\rho_1 + (1-\lambda)\rho_2, \sigma) \leq \lambda d(\rho_1, \sigma) + (1-\lambda)d(\rho_2, \sigma). \quad (33)$$

Given such a convex distance  $d$ , we extend the pure-state quantum  $t$ -AC measure to mixed states via the convex-roof construction:

$$\mathcal{A}_t^{Q,d}(\rho) = \min_{\{p_i, |\psi_i\rangle\}} \sum_i p_i \mathcal{A}_t^d(|\psi_i\rangle), \quad (34)$$

where the minimization is taken over all pure-state decompositions of  $\rho$ , and  $\mathcal{A}_t^d$  denotes the pure-state  $t$ -AC measure induced by the distance  $d$ . When the pure-state functional  $\mathcal{A}_t^d(|\psi\rangle)$  is an entanglement monotone across the bipartition  $t|N-t$ , its convex-roof extension provides a valid quantum  $t$ -AC measure associated with the corresponding total distance-based quantity.

**Proposition 6** (Proof in Appendix A6). *For any distance  $d$  whose associated total quantity  $\mathcal{A}_t^{T,d}$  satisfies the total-measure axioms, and for which the pure-state functional  $\mathcal{A}_t^d(|\psi\rangle)$  is an entanglement monotone across the*

$t | N-t$  bipartition, the convex-roof extension  $\mathcal{A}_t^{Q,d}$  satisfies axioms (Q1)–(Q5). If, in addition,  $\mathcal{A}_t^{T,d}$  is concave on  $\mathcal{D}(\mathcal{H}_j)$ , then the ordering axiom (Q6) also holds. Under these assumptions,  $\mathcal{A}_t^{Q,d}$  defines a quantum measure of  $t$ -AC associated with the corresponding total distance-based measure  $\mathcal{A}_t^{T,d}$ .

### 3. Fidelity-based construction

We now define the quantum measure associated with the total fidelity-based quantity (27). The key point is that, on pure states, the fidelity appearing in (26) is directly related to the negativity across the bipartition  $t | N-t$ . Applying Proposition 3 with  $d_A = t + 1$  gives, for every pure symmetric state  $|\psi\rangle$ ,

$$F(\rho_t, \rho_0^{(t)}) = \frac{1 + 2\mathcal{N}_t(|\psi\rangle)}{t + 1}. \quad (35)$$

Consequently,

$$\mathcal{A}_t^{T,F}(|\psi\rangle) = \frac{2}{t} \mathcal{N}_t(|\psi\rangle). \quad (36)$$

This suggests defining the associated quantum  $t$ -AC measure by the normalized convex-roof negativity

$$\mathcal{A}_t^{Q,F}(\rho) = \frac{2}{t} \mathcal{N}_t^{\text{CR}}(\rho), \quad (37)$$

where

$$\mathcal{N}_t^{\text{CR}}(\rho) = \min_{\{p_i, |\psi_i\rangle\}} \sum_i p_i \mathcal{N}_t(|\psi_i\rangle) \quad (38)$$

is the convex-roof extension of the negativity across the  $t | N-t$  bipartition [52].

**Proposition 7** (Proof in Appendix A 7). *The fidelity-based total candidate  $\mathcal{A}_t^{T,F}$  and the quantum quantity  $\mathcal{A}_t^{Q,F}$  defined in Eqs. (27) and (37) satisfy the following properties: The total candidate  $\mathcal{A}_t^{T,F}$  satisfies axioms (T1)–(T3); numerical evidence suggests that it also satisfies axiom (T4), but we leave this point open. The quantum quantity  $\mathcal{A}_t^{Q,F}$  satisfies axioms (Q1), (Q3)–(Q5), coincides with  $\mathcal{A}_t^{T,F}$  on pure states as required by (Q2), and obeys the ordering axiom (Q6) with respect to this total candidate. In particular,*

$$\mathcal{A}_t^{Q,F}(\rho) \leq \mathcal{A}_t^{T,F}(\rho) \quad \forall \rho \in \mathcal{D}(\mathcal{H}_j). \quad (39)$$

*Final remarks.* The previous propositions show that, for the purity-based and Hilbert–Schmidt distance-based constructions, the corresponding quantum measures satisfy axioms (Q1)–(Q6) relative to the chosen total measure. For the fidelity-based construction, the quantum quantity satisfies the quantum-side axioms and the ordering  $\mathcal{A}_t^{Q,F} \leq \mathcal{A}_t^{T,F}$  relative to the total candidate (27), so the corresponding classical contribution  $\mathcal{A}_t^{C,F} =$

$\mathcal{A}_t^{T,F} - \mathcal{A}_t^{Q,F}$  is nonnegative. However, since axiom (T4) for  $\mathcal{A}_t^{T,F}$  is supported here only by numerical evidence, the fidelity-based pair should be regarded as a well-motivated candidate total-quantum pair until a proof of total monotonicity under all  $\text{SU}(2)$ -covariant channels is obtained.

## C. Cumulative-multipole constructions

Cumulative multipole measures introduced and studied in [3, 38, 39, 53, 54] provide a tensor-based characterization of the angular structure of spin states. Related work connects these multipoles with higher-order polarization coherences and quantum polarization structure [53, 54]. In particular, they recover the standard distinction between first-order (Stokes-vector) polarization and higher-order, “hidden” angular structure by varying the cutoff rank: the case  $t = 1$  isolates first-order directional content, while  $t \geq 2$  probes the presence (or suppression) of higher-order multipoles. In our setting, this same hierarchy fits naturally with mixed-state total anticoherence, and could be further refined by separating, for each  $t$ , the total isotropy into quantum and classical contributions.

From the irreducible tensor-operator expansion (2), define the rank- $L$  multipole weight and its cumulative version by

$$C_{\leq t}(\rho) = \sum_{L=1}^t \sum_{M=-L}^L |\rho_{LM}|^2. \quad (40)$$

One has  $C_{\leq t}(\rho) = 0$  iff  $\rho$  is  $t$ -AC, i.e. all multipoles up to rank  $t$  vanish. Moreover, the multipole weights  $\sum_{M=-L}^L |\rho_{LM}|^2$  can be expressed as linear combinations of the reduced-state purities  $\text{Tr}(\rho_k^2)$  (see [11]), which makes explicit the link with the purity-based constructions.

### 1. Total cumulative-multipole AC

For  $1 \leq t \leq 2j - 1$ , a natural total  $t$ -anticoherence measure is obtained by an affine decreasing rescaling of  $C_{\leq t}$  that vanishes on pure coherent states. For spin-coherent states  $\rho_{\text{coh}} = |\theta, \phi\rangle\langle\theta, \phi|$ , one finds (independently of  $\theta, \phi$ )

$$C_{\leq t}(\rho_{\text{coh}}) = \frac{2j}{2j + 1} - \frac{((2j)!)^2}{(2j - t - 1)!(2j + t + 1)!}. \quad (41)$$

In this subsection, we therefore restrict ourselves to  $1 \leq t \leq 2j - 1$  and define

$$\mathcal{A}_t^{T,\text{cm}}(\rho) = 1 - \frac{C_{\leq t}(\rho)}{C_{\leq t}(\rho_{\text{coh}})}. \quad (42)$$

**Proposition 8** (Proof in Appendix A 8). *For  $1 \leq t \leq 2j - 1$ , the quantity  $\mathcal{A}_t^{T,\text{cm}}$  satisfies axioms (T1)–(T4), and therefore defines a valid measure of total  $t$ -anticoherence.*

## 2. Quantum cumulative-multipole AC ?

A natural attempt at defining a corresponding *quantum* cumulative-multipole measure is to take the convex roof of the pure-state functional:

$$\mathcal{A}_t^{Q,\text{cm}}(\rho) = \min_{\{p_i, |\psi_i\rangle\}} \sum_i p_i \mathcal{A}_t^{T,\text{cm}}(|\psi_i\rangle\langle\psi_i|). \quad (43)$$

However, even though  $\mathcal{A}_t^{Q,\text{cm}}$  satisfies axioms (Q1)–(Q4) and (Q6), it fails to satisfy the axiom (Q5) about monotonicity under LOCC operations for  $t \geq 2$ , and therefore does not define a valid quantum AC measure. This already occurs at the pure-state level as the following example shows.

Consider the spin-2 pure states

$$|\psi\rangle = \frac{1}{\sqrt{3}}(|2, 2\rangle + |2, 0\rangle + |2, -2\rangle), \quad (44)$$

$$|\phi\rangle = \frac{1}{\sqrt{6}}(-2|2, 2\rangle - |2, 0\rangle + |2, -2\rangle). \quad (45)$$

Across the bipartition  $2|2$ , their Schmidt spectra are

$$\lambda(\psi) = \left( \frac{7}{18} + \frac{\sqrt{6}}{9}, \frac{2}{9}, \frac{7}{18} - \frac{\sqrt{6}}{9} \right), \quad (46)$$

$$\lambda(\phi) = \left( \frac{4}{9} + \frac{\sqrt{87}}{36}, \frac{4}{9} - \frac{\sqrt{87}}{36}, \frac{1}{9} \right). \quad (47)$$

These satisfy  $\lambda(\psi) \prec \lambda(\phi)$ . Hence, by Nielsen's theorem [55], there exists a deterministic LOCC transformation  $|\psi\rangle \rightarrow |\phi\rangle$  across the split  $2|2$ .

We now evaluate the cumulative multipole measure directly from Eq. (42) for  $t = 2$  and obtain

$$\mathcal{A}_2^{T,\text{cm}}(|\psi\rangle\langle\psi|) = \frac{7}{12}, \quad \mathcal{A}_2^{T,\text{cm}}(|\phi\rangle\langle\phi|) = \frac{31}{48}. \quad (48)$$

Since both states are pure, their total AC measure is equal to their quantum AC measure, and thus

$$\mathcal{A}_2^{Q,\text{cm}}(|\psi\rangle\langle\psi|) = \frac{7}{12} < \frac{31}{48} = \mathcal{A}_2^{Q,\text{cm}}(|\phi\rangle\langle\phi|), \quad (49)$$

although  $|\psi\rangle \rightarrow |\phi\rangle$  is achievable by deterministic LOCC. This shows that the quantum cumulative-multipole measure violates axiom (Q5) for  $t = 2$ . Similarly, one can find examples of violations for  $t > 2$ . It is only for  $t = 1$  that (Q5) holds due to the following Proposition.

**Proposition 9** (Proof in Appendix A 9). *For  $t = 1$ , the cumulative-multipole and purity-based constructions are affinely equivalent on pure states. Consequently, their convex-roof quantum extensions coincide:*

$$\mathcal{A}_1^{Q,\text{cm}}(\rho) = \mathcal{A}_1^{Q,\mathcal{P}}(\rho) \quad \forall \rho \in \mathcal{D}(\mathcal{H}_j), \quad (50)$$

with the normalizations chosen above. In particular,  $\mathcal{A}_1^{Q,\text{cm}}$  satisfies axiom (Q5).

## IV. EVALUATION OF MEASURES

*Example 1. Rank-2 mixed states for  $j = 2$*

As a first explicit illustration of the interplay between total, quantum, and classical anticoherece, we consider a rank-2 mixed state of a spin-2 system, corresponding to  $N = 2j = 4$  qubits,

$$\rho(\lambda) = \lambda |\psi_+\rangle\langle\psi_+| + (1 - \lambda) |\psi_-\rangle\langle\psi_-|, \quad (51)$$

where the orthonormal eigenvectors are given by

$$|\psi_\pm\rangle = \frac{1}{2}(|2, 2\rangle \pm i\sqrt{2} |2, 0\rangle + |2, -2\rangle). \quad (52)$$

*Fidelity-based measure for  $t = 1$ .* For arbitrary weight  $\lambda$ , the partial transposes  $(|\psi_\pm\rangle\langle\psi_\pm|)^{T_1}$  have supports on orthogonal subspaces. As a consequence, the negativity is additive on the spectral decomposition of  $\rho$ , i.e.,

$$\mathcal{N}_1(\rho) = \lambda \mathcal{N}_1(|\psi_+\rangle) + (1 - \lambda) \mathcal{N}_1(|\psi_-\rangle). \quad (53)$$

Since each eigenvector is maximally 1-AC,  $\mathcal{N}_1(|\psi_\pm\rangle) = 1/2$ , it follows immediately that

$$\mathcal{N}_1^{\text{CR}}(\rho) = \mathcal{N}_1(\rho) = \frac{1}{2}, \quad (54)$$

independently of the mixing parameter  $\lambda$ . Using the definition of the fidelity-based quantum measure then yields

$$\mathcal{A}_1^{Q,F}(\rho) = 1. \quad (55)$$

Since the total measure also equals unity for  $t = 1$ , one has

$$\mathcal{A}_1^{T,F}(\rho) = \mathcal{A}_1^{Q,F}(\rho) = 1, \quad \mathcal{A}_1^{C,F}(\rho) = 0. \quad (56)$$

This provides an explicit example of a *mixed* state that is perfectly 1-AC with a purely quantum origin. Such states have appeared previously in the literature. In particular, the vectors (52) span a 1-AC *subspace*, meaning that every pure state in their span is 1-AC [29, 56].

*Purity-based measure for  $t = 2$ .* We consider the same example as above. A direct evaluation of the reduced two-qubit state  $\rho_2$  gives  $\text{Tr} \rho_2^2 = \frac{1}{3}$ ; hence, the total purity-based measure is  $\mathcal{A}_2^{T,\mathcal{P}}(\rho) = 1$ , independently of  $\lambda$ . We now determine the convex-roof quantum contribution. Since  $\rho$  has rank 2, we may identify its support with an effective qubit spanned by  $\{|\psi_+\rangle, |\psi_-\rangle\}$  and write  $\rho$  in Bloch form with  $\mathbf{r} = (0, 0, r_z)$ ,  $r_z = 2\lambda - 1$ . Any decomposition  $\rho = \sum_i p_i |\phi_i\rangle\langle\phi_i|$  corresponds to an ensemble of pure Bloch vectors  $\mathbf{n}_i$  with  $\sum_i p_i \mathbf{n}_i = \mathbf{r}$ , and therefore  $\sum_i p_i z_i = r_z$ , where  $z_i$  denotes the  $z$ -component of  $\mathbf{n}_i$ .

For a pure state  $|\phi\rangle$  in the support, the purity-based functional can be written as

$$\mathcal{A}_2^{\mathcal{P}}(|\phi\rangle) = \frac{3 + z^2}{4}, \quad (57)$$

Hence, for an arbitrary decomposition,

$$\begin{aligned} \sum_i p_i \mathcal{A}_2^{\mathcal{P}}(|\phi_i\rangle) &= \frac{3}{4} + \frac{1}{4} \sum_i p_i z_i^2 \\ &\geq \frac{3}{4} + \frac{1}{4} \left( \sum_i p_i z_i \right)^2 = \frac{3 + r_z^2}{4}, \end{aligned} \quad (58)$$

where we used Jensen's inequality for the convex function  $z^2$ . The bound is tight. For  $r_z = 2\lambda - 1$ , choose  $\theta$  such that  $\cos \theta = r_z$  and define

$$|\phi_{\pm}\rangle = \cos \frac{\theta}{2} |\psi_+\rangle \pm \sin \frac{\theta}{2} |\psi_-\rangle. \quad (59)$$

Then  $\rho = \frac{1}{2} |\phi_+\rangle \langle \phi_+| + \frac{1}{2} |\phi_-\rangle \langle \phi_-|$ , and both  $|\phi_{\pm}\rangle$  have the same Bloch  $z$ -component  $z_{\pm} = r_z$ , so the Jensen bound is saturated. Therefore,

$$\mathcal{A}_2^{\mathcal{Q},\mathcal{P}}(\rho) = \frac{3 + r_z^2}{4} = \frac{3 + (2\lambda - 1)^2}{4} = \lambda^2 - \lambda + 1. \quad (60)$$

Finally, the corresponding classical contribution is

$$\mathcal{A}_2^{C,\mathcal{P}}(\rho) = \mathcal{A}_2^{T,\mathcal{P}}(\rho) - \mathcal{A}_2^{\mathcal{Q},\mathcal{P}}(\rho) = \lambda(1 - \lambda), \quad (61)$$

which vanishes for  $\lambda \in \{0, 1\}$  and is maximal for the equal mixture  $\lambda = 1/2$ . This result is illustrated in Figure 1.

*Purity-based measure for  $t = 3$ .* For  $t = 3$ , an analogous calculation gives

$$\mathcal{A}_3^{\mathcal{Q},\mathcal{P}}(\rho) = \frac{2}{3}, \quad (62)$$

which is independent of  $\lambda$ . The total measure, however, now depends on the mixing parameter and reads

$$\mathcal{A}_3^{T,\mathcal{P}}(\rho) = \frac{2}{3}(-2\lambda^2 + 2\lambda + 1). \quad (63)$$

The classical contribution is thus

$$\mathcal{A}_3^{C,\mathcal{P}}(\rho) = \mathcal{A}_3^{T,\mathcal{P}}(\rho) - \mathcal{A}_3^{\mathcal{Q},\mathcal{P}}(\rho) = \frac{4}{3}\lambda(1 - \lambda). \quad (64)$$

*Fidelity-based measures for  $t = 2, 3$ .* The fidelity-based measures can also be evaluated analytically for this family. For  $t = 2$ , the reduced state is maximally mixed for all  $\lambda$ , so

$$\mathcal{A}_2^{T,F}(\rho) = 1. \quad (65)$$

It remains to evaluate the convex-roof negativity. Let  $z = 2\lambda - 1$  and identify the support of  $\rho$  with a qubit. For a pure state  $|\phi\rangle = \alpha|\psi_+\rangle + \beta|\psi_-\rangle$ , define

$$x = 2 \operatorname{Re}(\alpha^* \beta), \quad y = 2 \operatorname{Im}(\alpha^* \beta), \quad z_{\phi} = |\alpha|^2 - |\beta|^2. \quad (66)$$

The spectrum of the two-qubit reduced state is

$$p_{\pm} = \frac{1}{3} + \frac{x}{6} \pm \frac{\sqrt{3}y}{6}, \quad p_3 = \frac{1}{3} - \frac{x}{3}, \quad (67)$$

and therefore

$$\mathcal{A}_2^F(|\phi\rangle) = \mathcal{N}_2(|\phi\rangle) = \sqrt{p_+ p_-} + \sqrt{p_+ p_3} + \sqrt{p_- p_3}. \quad (68)$$

An elementary minimization over  $x, y$  at fixed  $z_{\phi}$  gives

$$\mathcal{A}_2^F(|\phi\rangle) \geq \frac{1 + |z_{\phi}|}{2}. \quad (69)$$

Consequently, consider an arbitrary pure-state decomposition  $\rho(\lambda) = \sum_i p_i |\phi_i\rangle \langle \phi_i|$ , with  $|\phi_i\rangle = \alpha_i |\psi_+\rangle + \beta_i |\psi_-\rangle$ . Since this decomposition must reproduce the Bloch vector of  $\rho(\lambda)$  inside the support  $\operatorname{span}\{|\psi_+\rangle, |\psi_-\rangle\}$ , its  $z$ -components satisfy

$$\sum_i p_i z_i = 2\lambda - 1, \quad z_i = |\alpha_i|^2 - |\beta_i|^2. \quad (70)$$

Using the bound above for each pure state in the decomposition, we obtain

$$\begin{aligned} \sum_i p_i \mathcal{A}_2^F(|\phi_i\rangle) &\geq \frac{1}{2} + \frac{1}{2} \sum_i p_i |z_i| \\ &\geq \frac{1}{2} + \frac{1}{2} \left| \sum_i p_i z_i \right| \\ &= \frac{1}{2} + \left| \lambda - \frac{1}{2} \right|. \end{aligned} \quad (71)$$

This lower bound is tight. For  $\lambda \geq 1/2$ , write

$$\rho(\lambda) = (2\lambda - 1)|\psi_+\rangle \langle \psi_+| + 2(1 - \lambda)\rho_*, \quad (72)$$

where

$$\rho_* = \frac{1}{2} (|\psi_+\rangle \langle \psi_+| + |\psi_-\rangle \langle \psi_-|) = \frac{1}{3} \sum_{k=0}^2 |\phi_k\rangle \langle \phi_k| \quad (73)$$

with

$$|\phi_k\rangle = \frac{1}{\sqrt{2}} \left( |\psi_+\rangle + e^{2\pi i k/3} |\psi_-\rangle \right). \quad (74)$$

Since  $\mathcal{A}_2^F(|\psi_+\rangle) = 1$  and  $\mathcal{A}_2^F(|\phi_k\rangle) = 1/2$ , this decomposition has average value  $\lambda$ . The case  $\lambda \leq 1/2$  is obtained by exchanging  $|\psi_+\rangle$  and  $|\psi_-\rangle$ . Hence

$$\mathcal{A}_2^{\mathcal{Q},F}(\rho) = \frac{1}{2} + \left| \lambda - \frac{1}{2} \right|, \quad \mathcal{A}_2^{C,F}(\rho) = \frac{1}{2} - \left| \lambda - \frac{1}{2} \right|. \quad (75)$$

For  $t = 3$ , the reduced state  $\rho_3$  has spectrum

$$\left\{ \frac{\lambda}{2}, \frac{\lambda}{2}, \frac{1 - \lambda}{2}, \frac{1 - \lambda}{2} \right\}, \quad (76)$$

which gives

$$\mathcal{A}_3^{T,F}(\rho) = \frac{1 + 4\sqrt{\lambda(1 - \lambda)}}{3}. \quad (77)$$

Moreover, every pure state in the support has the same negativity across the 3|1 bipartition, namely  $\mathcal{N}_3 = 1/2$ . Thus

$$\mathcal{A}_3^{\mathcal{Q},F}(\rho) = \frac{1}{3}, \quad \mathcal{A}_3^{C,F}(\rho) = \frac{4}{3} \sqrt{\lambda(1 - \lambda)}. \quad (78)$$

Together with the purity-based expressions above, these analytical results are shown in Fig. 1.

This example clearly illustrates how increasing the order  $t$  enhances the relative weight of the classical contribution to isotropy. While 1-anticoherence is entirely quantum and robust under mixing, higher-order anticoherence increasingly relies on probabilistic mixing, even though the total isotropy may remain high.

### A. States saturating the convex-roof negativity

For the quantum AC measure associated with the fidelity-based construction, one must calculate the convex-roof extension of the negativity  $\mathcal{N}_t^{\text{CR}}(\rho)$ . Here, we discuss two cases where this quantity can be computed explicitly.

#### 1. Mixed states with support of equal negativity

The first case is when every state in the support of  $\rho$  has the same negativity. In this case, it is immediate to obtain that for any pure decomposition of  $\rho = \sum_i p_i |\psi_i\rangle\langle\psi_i|$ ,  $\sum_i p_i \mathcal{N}(|\psi_i\rangle)$  has the same value. Consequently, there is no need to do a minimization to evaluate  $\mathcal{N}_t^{\text{CR}}(\rho)$ . In particular, one can directly calculate it from the eigenbasis of the state  $\mathcal{N}_t^{\text{CR}}(\rho) = \sum_i \lambda_i \mathcal{N}(|\phi_i\rangle)$ .

This situation occurs for mixed states whose support lies in a  $t$ -AC subspace. By definition, any state in a  $t$ -AC subspace is  $t$ -AC [29, 56]. Moreover, a  $t$ -AC pure state has maximum negativity  $\mathcal{N}_t(|\psi\rangle) = t/2$  ( $t \leq N/2$ ) [29, 41]. Whenever the support of a mixed state is itself a  $t$ -AC subspace, the resulting state displays maximal quantum  $t$ -anticoherence, independently of the specific mixing probabilities.

**Theorem 1.** *Let  $\rho$  be a mixed spin- $j$  state whose image<sup>6</sup>  $\text{Im}(\rho) \subset \mathcal{H}_j$  is a  $t$ -AC subspace. Then every pure state in every decomposition of  $\rho$  belongs to this subspace and is  $t$ -AC. Hence each such pure state has maximal negativity  $\mathcal{N}_t = t/2$  across the  $t | N-t$  bipartition, and the convex-roof negativity is*

$$\mathcal{N}_t^{\text{CR}}(\rho) = t/2. \quad (79)$$

Consequently, the associated quantum  $t$ -anticoherence measure attains its maximal value,  $\mathcal{A}_t^{\text{Q},F}(\rho) = 1$ . If the stronger ordinary-negativity equality  $\mathcal{N}_t(\rho) = t/2$  holds for a particular  $t$ -AC subspace, as in the settings characterized in Ref. [29], then the ordinary negativity and the convex-roof negativity coincide for such states.

<sup>6</sup> The image of an operator is the subspace spanned by its eigenvectors with nonzero eigenvalues.

Since the total  $t$ -anticoherence is also maximal for such states, the classical contribution necessarily vanishes. Therefore, any mixed state supported on a  $t$ -AC subspace exhibits *purely quantum*  $t$ -anticoherence, extending to mixed states a property previously known for pure AC states.

#### Example 2. 2-AC subspaces for $N = 7$

As a second example, consider the symmetric  $N = 7$  qubit states [57, 58]

$$\begin{aligned} |\psi_1\rangle &= \sqrt{\frac{3}{10}} \left| \frac{7}{2}, \frac{7}{2} \right\rangle + \sqrt{\frac{7}{10}} \left| \frac{7}{2}, -\frac{3}{2} \right\rangle, \\ |\psi_2\rangle &= \sqrt{\frac{7}{10}} \left| \frac{7}{2}, \frac{3}{2} \right\rangle - \sqrt{\frac{3}{10}} \left| \frac{7}{2}, -\frac{7}{2} \right\rangle. \end{aligned} \quad (80)$$

These vectors span a 2-AC subspace. Therefore, for any mixture  $\rho$  supported on this subspace one finds

$$\mathcal{N}_1^{\text{CR}}(\rho) = \frac{1}{2}, \quad \mathcal{N}_2^{\text{CR}}(\rho) = 1, \quad (81)$$

and hence  $\mathcal{A}_t^{T,F}(\rho) = \mathcal{A}_t^{Q,F}(\rho) = 1$  for  $t = 1, 2$ .

#### 2. Pairwise orthogonal partial transposed projectors

By definition, the negativity satisfies

$$\mathcal{N}_t^{\text{CR}}(\rho) \geq \mathcal{N}_t(\rho). \quad (82)$$

A sufficient condition for saturation is the following: consider a decomposition of the state  $\rho = \sum_i p_i |\psi_i\rangle\langle\psi_i|$ . If the images of the partially transposed projectors  $(|\psi_i\rangle\langle\psi_i|)^{TA}$  are pairwise orthogonal subspaces<sup>7</sup>, then the negativity is additive over the decomposition<sup>8</sup>,

$$\sum_i p_i \mathcal{N}_t(|\psi_i\rangle) = \mathcal{N}_t(\rho). \quad (83)$$

In this case, the given decomposition is optimal for the convex-roof construction. Indeed, the given decomposition yields

$$\mathcal{N}_t(\rho) \leq \mathcal{N}_t^{\text{CR}}(\rho) \leq \sum_i p_i \mathcal{N}_t(|\psi_i\rangle) = \mathcal{N}_t(\rho), \quad (84)$$

so equality holds throughout, and the convex roof is easily evaluated. Such orthogonality among the partially transposed operators also appears in the orthogonal basis of

<sup>7</sup> Two subspaces are orthogonal if every vector in one is orthogonal to every vector in the other.

<sup>8</sup> This follows from the following result: let  $A$  and  $B$  be two diagonalizable matrices, and let  $\lambda_{\neq 0}(A)$  be the set of nonzero eigenvalues (counting multiplicity) of  $A$ . Then,  $\lambda_{\neq 0}(A+B) = \lambda_{\neq 0}(A) \cup \lambda_{\neq 0}(B)$  if  $\text{im}(A) \perp \text{im}(B)$ . In particular, when this holds, the negative eigenvalues of  $A+B$  are the union of the negative eigenvalues of  $A$  and  $B$ .

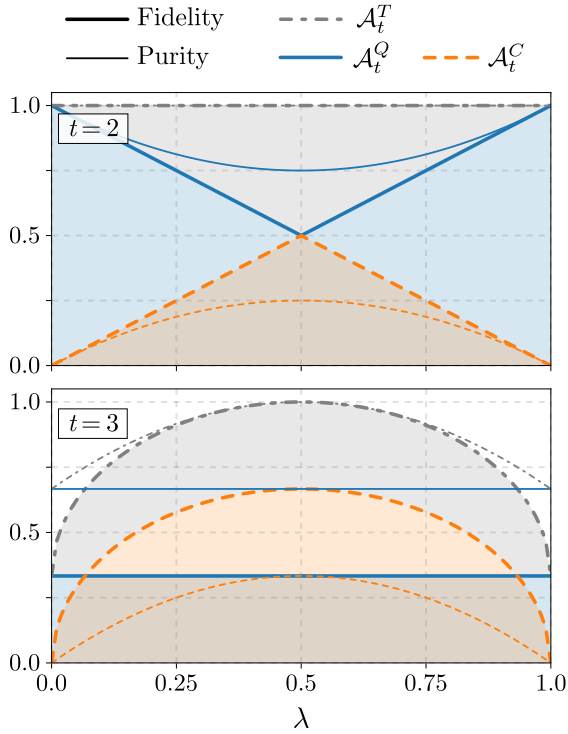


Figure 1. Total, quantum, and classical  $t$ -anticoherence of the mixed state (51) as functions of the mixing weight  $\lambda$ . The upper and lower panels correspond to  $t = 2$  and  $t = 3$ , respectively. Thick curves correspond to the fidelity-based definitions (27) and (37), evaluated analytically in Sec. IV; thin curves show the purity-based measures. In particular,  $\mathcal{A}_2^{Q,F} = \frac{1}{2} + |\lambda - \frac{1}{2}|$  and  $\mathcal{A}_3^{Q,F} = \frac{1}{3}$ . For  $t = 1$ , both measures give  $\mathcal{A}_1^T = \mathcal{A}_1^Q = 1$  and  $\mathcal{A}_1^C = 0$  (data not shown).

an AC subspace (see Appendix F in Ref. [29]). However, they are not the only cases. Another nontrivial example that does not arise from an AC subspace is given by two spin-5/2 states:

$$\begin{aligned} |\psi_1\rangle &= \frac{1}{\sqrt{6}} \left| \frac{5}{2}, -\frac{5}{2} \right\rangle + \sqrt{\frac{5}{6}} \left| \frac{5}{2}, \frac{3}{2} \right\rangle, \\ |\psi_2\rangle &= -\sqrt{\frac{5}{6}} \left| \frac{5}{2}, -\frac{3}{2} \right\rangle + \frac{1}{\sqrt{6}} \left| \frac{5}{2}, \frac{5}{2} \right\rangle. \end{aligned} \quad (85)$$

In their representation as  $N = 5$  symmetric qubits, and considering the partial transposed density matrices in the bipartition  $t|N - t$  with  $t = 1$ , we obtain that  $(|\psi_1\rangle\langle\psi_1|)^{TA} \perp (|\psi_2\rangle\langle\psi_2|)^{TA}$ . Therefore,

$$\begin{aligned} \mathcal{N}_1^{\text{CR}}(\lambda|\psi_1\rangle\langle\psi_1| + (1-\lambda)|\psi_2\rangle\langle\psi_2|) \\ = \lambda\mathcal{N}_1(|\psi_1\rangle) + (1-\lambda)\mathcal{N}_1(|\psi_2\rangle) = \frac{\sqrt{2}}{3}. \end{aligned}$$

## V. APPLICATIONS

### A. Robustness of quantum AC under particle loss

Figure 2 compares the robustness of the quantum, purity-based  $t$ -anticoherence  $\mathcal{A}_t^{Q,\mathcal{P}}$  under particle loss for three emblematic families of symmetric  $N$ -qubit pure states: highest-order anticoherent pure (HOAP) states [41],  $W$  states, and GHZ states. For each  $N$  and each remaining subsystem size  $q$ , we consider the reduced state  $\rho_q = \text{Tr}_{N-q}(|\psi\rangle\langle\psi|)$  and evaluate  $\mathcal{A}_t^{Q,\mathcal{P}}(\rho_q)$  for  $t = 1$  (left column) and  $t = 2$  (right column) [59].

Two qualitative behaviors stand out. First, HOAP states, which are AC of order  $t \geq 2$  for  $N = 4$  and  $N \geq 6$ , retain a large *quantum* anticoherence for moderate particle losses:  $\mathcal{A}_t^{Q,\mathcal{P}}(\rho_q)$  remains high as long as a significant fraction of the particles is conserved and only becomes negligible once approximately half (or more) of the system is traced out. In this regime, the anticoherence of reduced states becomes mainly classical, in the sense that any remaining lower-order isotropy is not supported by quantum correlations across the relevant bipartitions. Second, this behavior contrasts sharply with 1-AC GHZ states: their quantum anticoherence is extremely fragile, collapsing as soon as any particle is traced out. In Fig. 2, this appears as nonzero values only on the “no-loss” diagonal  $q = N$ , while reduced states with  $q < N$  exhibit  $\mathcal{A}_t^{Q,\mathcal{P}} = 0$ . This is consistent with the well-known fact that particle loss destroys the entanglement structure of GHZ states, rendering the reduced states separable. Finally,  $W$  states, which are not exactly  $t$ -AC in the orders considered here, show the most persistent quantum anticoherence under loss:  $\mathcal{A}_t^{Q,\mathcal{P}}(\rho_q)$  remains visibly nonzero over a broad range of  $q$ , even when many particles are discarded. This robustness comes at the price of not reaching maximal quantum anticoherence: compared with HOAP states, the values are typically smaller (moderate marker sizes and intermediate colors), indicating a more uniform but partial quantum contribution to isotropy.

### B. Maximal anticoherence order for mixed states at fixed purity

For mixed states, anticoherence competes with purity: increasing isotropy generally requires mixing, while higher purity constrains the degree to which low-order spin moments can be suppressed. A natural question is therefore the following: *given a fixed global purity, what is the maximal order  $t$  of anticoherence that a mixed spin state can achieve?*

This question is particularly relevant from the perspective of quantum resources. At fixed purity, different states may display the same total amount of isotropy while differing markedly in the relative contributions arising from genuinely quantum correlations and from sta-

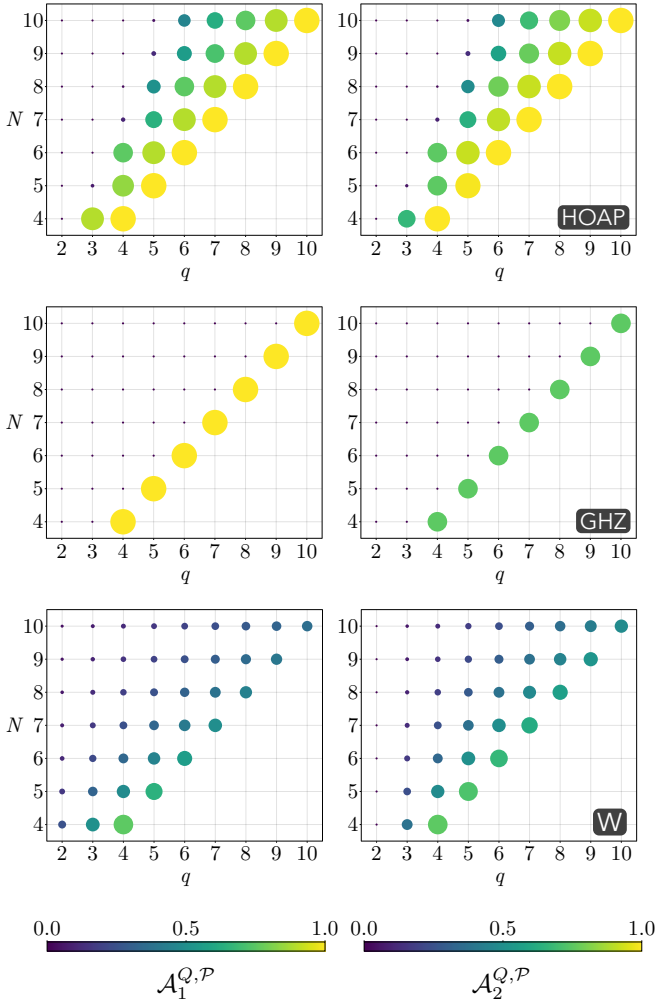


Figure 2. Quantum purity-based  $t$ -anticoherece of reduced  $q$ -qubit states (seen as spin- $q/2$  states). Left (right):  $t = 1$  ( $t = 2$ ). Reduced states are obtained by partial tracing HOAP states [41] (top), GHZ states (middle), and  $W$  states (bottom). Disk areas scale with the magnitude of  $\mathcal{A}_t^{Q,\mathcal{P}}$ ; dark-purple disks of minimal size indicate vanishing anticoherece.

tistical mixing. Our framework allows one to resolve this distinction by separating total, quantum, and classical contributions to  $t$ -anticoherece.

For non-symmetric multipartite systems, related trade-offs between purity and isotropy have been investigated in Ref. [60]. Here, we use the same type of techniques based on semidefinite programming but adapted to symmetric states and characterise the maximum achievable anticoherece order as a function of purity within this physically relevant sector.

Figure 3 summarizes our results for  $j = 3/2, 2$  and  $5/2$ . For each value of the purity, we identify mixed states that are exactly  $t$ -AC, and hence maximize any admissible total  $t$ -AC measure by axiom (T1); we then indicate the highest such order  $t$ . The accompanying pie charts display the relative contributions of quantum ( $\mathcal{A}_t^{Q,\mathcal{P}}$ ) and classical ( $\mathcal{A}_t^{C,\mathcal{P}}$ ) anticoherece at that order.

A completely filled chart corresponds to a perfectly  $t$ -AC state. The highest achievable order  $t$  is piecewise constant: as  $\text{Tr}(\rho^2)$  decreases, successive thresholds are crossed where an additional multipolar rank can be completely removed, and the maximum achievable order increases by one step (blue staircase curve). To achieve higher orders of total anticoherece, the mixture must be increased: total isotropy at high  $t$  is only accessible when the purity is sufficiently low. Along this staircase, the *composition* of the isotropy changes: the charts indicate that the quantum contribution  $\mathcal{A}_t^{Q,\mathcal{P}}$  (blue) generally decreases as  $t$  increases, while the complementary classical contribution  $\mathcal{A}_t^{C,\mathcal{P}}$  (orange) increases. In other words, reducing the purity allows for stronger total isotropy, but an increasing fraction of this isotropy comes from statistical mixing rather than genuine quantum correlations.

We complement Fig. 3 with explicit mixed states realizing the different steps of the purity–AC trade-off. These examples serve two purposes. First, they show that the bounds are not merely numerical: the extremal points can be attained by simple low-rank mixtures in the Dicke basis. Second, they illustrate how the nature of isotropy changes with the order  $t$ . For each state and each relevant order, Table I reports the triple  $(\mathcal{A}_t^{T,\mathcal{P}}, \mathcal{A}_t^{Q,\mathcal{P}}, \mathcal{A}_t^{C,\mathcal{P}})$ , together with the rank and the global purity. The general trend is that reaching higher orders of total AC at fixed spin requires higher rank and more mixing, and the additional isotropy is increasingly classical. By contrast, a large quantum contribution is possible only at lower orders, or in the special case where the support of the mixed state forms a  $t$ -AC subspace.

The staircase in Fig. 3 should be interpreted as follows. The displayed jumps are certified by explicit feasible states given below and by semidefinite-programming searches in the symmetric sector. In these searches the  $t$ -AC constraints are imposed as the linear constraints  $\rho_t = \mathbb{1}_{t+1}/(t+1)$ , equivalently by the vanishing of the multipoles with  $1 \leq L \leq t$ . Since the global purity constraint  $\text{Tr}(\rho^2) = \text{const.}$  is quadratic, the numerical search is performed by optimizing linear objectives over fixed-rank or fixed-support ansatz families and by checking the achieved purities a posteriori. Thus the explicit states prove attainability of the indicated steps.

1.  $j = \frac{3}{2}$

The first nontrivial example occurs for  $j = 3/2$ . For pure spin-3/2 states, the maximal anticoherece order is only 1; reaching second-order isotropy therefore requires mixing. Consider the two orthonormal states

$$\begin{aligned} |\psi_1\rangle &= \frac{1}{\sqrt{2}}\left(\left|\frac{3}{2}, \frac{3}{2}\right\rangle + \left|\frac{3}{2}, -\frac{1}{2}\right\rangle\right), \\ |\psi_2\rangle &= \frac{1}{\sqrt{2}}\left(-\left|\frac{3}{2}, \frac{1}{2}\right\rangle + \left|\frac{3}{2}, -\frac{3}{2}\right\rangle\right). \end{aligned} \quad (86)$$

Their equal mixture,

$$\rho = \frac{1}{2}(|\psi_1\rangle\langle\psi_1| + |\psi_2\rangle\langle\psi_2|), \quad (87)$$

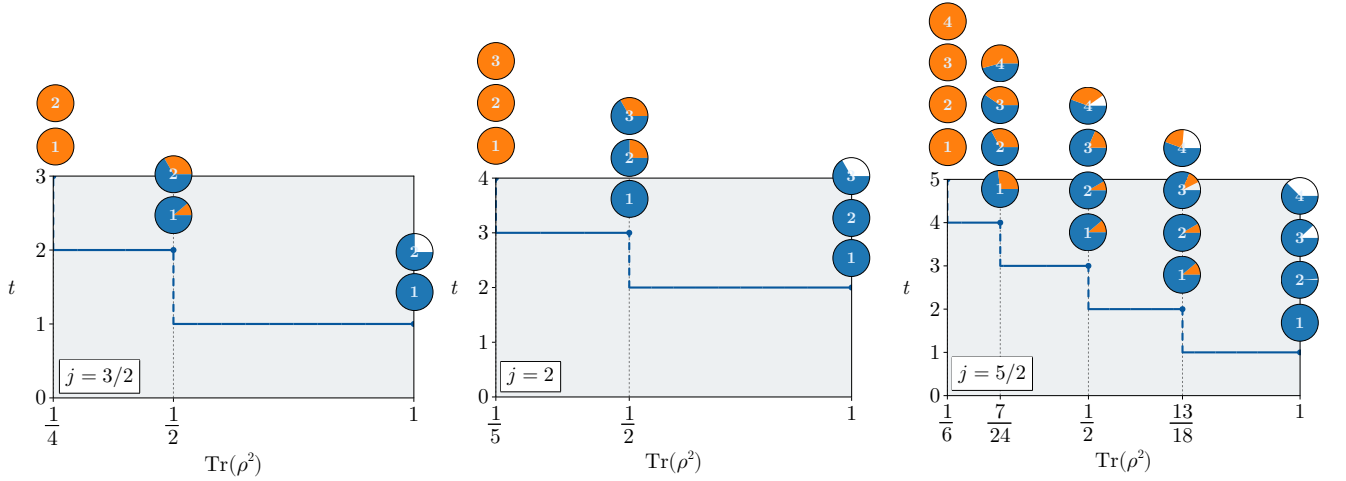


Figure 3. Maximal achievable total AC order as a function of the global purity. For each purity threshold, the pie chart shows the decomposition of the purity-based AC measure into its quantum contribution  $\mathcal{A}_t^{Q,P}$  (blue) and classical contribution  $\mathcal{A}_t^{C,P}$  (orange), evaluated at the maximal attainable order  $t$ . The number at the center of each pie gives this order. A fully filled pie indicates a state that is exactly  $t$ -AC. The states realizing the jumps are given in Eqs. (87), (89), (91), (92), and (94); see also Table I. The leftmost charts correspond to the MMS state, while the rightmost charts correspond to HOAP states [41].

has purity  $1/2$  and is exactly 2-AC. It thus provides the lowest-spin example in which mixing enables a higher anticoherece order than is possible for pure states.

### 2. $j = 2$

For  $j = 2$ , a rank-2 construction already reaches one order higher. Define

$$|\psi_{\pm}\rangle = \frac{1}{2}(|2, 2\rangle \pm i\sqrt{2}|2, 0\rangle + |2, -2\rangle). \quad (88)$$

The equal mixture

$$\rho = \frac{1}{2}(|\psi_+\rangle\langle\psi_+| + |\psi_-\rangle\langle\psi_-|) \quad (89)$$

has purity  $1/2$  and is exactly 3-AC. This example is particularly useful because the same two-dimensional support is also a 1-AC subspace, so first-order isotropy remains entirely quantum, while higher-order isotropy contains an increasing classical contribution (see the pie charts in the middle panel of Fig. 3).

### 3. $j = 5/2$

For  $j = 5/2$ , several extremal regimes can be realized depending on the rank and purity of the mixture (see Fig. 3, right panel).

*Rank-2 states.* Let

$$\begin{aligned} |\psi_1\rangle &= \frac{1}{\sqrt{2}}(|\tfrac{5}{2}, \tfrac{5}{2}\rangle + |\tfrac{5}{2}, -\tfrac{5}{2}\rangle), \\ |\psi_2\rangle &= \frac{1}{\sqrt{2}}(|\tfrac{5}{2}, \tfrac{3}{2}\rangle + |\tfrac{5}{2}, -\tfrac{3}{2}\rangle). \end{aligned} \quad (90)$$

The unequal mixture

$$\rho = \frac{1}{6}|\psi_1\rangle\langle\psi_1| + \frac{5}{6}|\psi_2\rangle\langle\psi_2| \quad (91)$$

has purity  $13/18$  and is exactly 2-AC. Thus, at relatively high purity, only low-order isotropy can be made perfect.

A lower-purity rank-2 mixture reaches third-order anticoherece. Let  $|\psi_1\rangle$  and  $|\psi_2\rangle$  be the states of Eq. (85). Then

$$\rho = \frac{1}{2}(|\psi_1\rangle\langle\psi_1| + |\psi_2\rangle\langle\psi_2|) \quad (92)$$

has purity  $1/2$  and is exactly 3-AC. Compared with the previous state, the additional order of isotropy is obtained by increasing the degree of mixing.

*Rank-4 state.* Finally, fourth-order anticoherece requires a still more mixed state. Let

$$\begin{aligned} |\psi_1\rangle &= |\tfrac{5}{2}, -\tfrac{1}{2}\rangle, \\ |\psi_2\rangle &= |\tfrac{5}{2}, -\tfrac{3}{2}\rangle, \\ |\psi_3\rangle &= \sqrt{\tfrac{9}{20}}|\tfrac{5}{2}, \tfrac{5}{2}\rangle + \sqrt{\tfrac{11}{20}}|\tfrac{5}{2}, -\tfrac{5}{2}\rangle, \\ |\psi_4\rangle &= |\tfrac{5}{2}, \tfrac{1}{2}\rangle. \end{aligned} \quad (93)$$

The rank-4 mixture

$$\rho = \frac{1}{12}|\psi_1\rangle\langle\psi_1| + \frac{1}{4}|\psi_2\rangle\langle\psi_2| + \frac{1}{3}(|\psi_3\rangle\langle\psi_3| + |\psi_4\rangle\langle\psi_4|) \quad (94)$$

has purity  $7/24$  and is exactly 4-AC. This example illustrates the general pattern most clearly: the highest anticoherece order is achieved only after substantial mixing, and the corresponding total isotropy is dominated by its classical component.

Table I summarizes the AC measures of the representative states discussed in Sec. VB.

## VI. CONCLUSIONS

We have developed a systematic framework to quantify spin anticoherece beyond the pure-state setting. In

$j$	State	Rank	Purity	$t$	$(\mathcal{A}_t^{T,\mathcal{P}}, \mathcal{A}_t^{Q,\mathcal{P}}, \mathcal{A}_t^{C,\mathcal{P}})$
$\frac{3}{2}$	(87)	2	$\frac{1}{2}$	1,2	$(1, \frac{8}{9}, \frac{1}{9}), (1, \frac{2}{3}, \frac{1}{3})$
2	(89)	2	$\frac{1}{2}$	1,2,3	$(1, 1, 0), (1, \frac{3}{4}, \frac{1}{4}), (1, \frac{2}{3}, \frac{1}{3})$
$\frac{5}{2}$	(91)	2	$\frac{13}{18}$	1,2,3,4	$(1, \frac{8}{9}, \frac{1}{9}), (1, \frac{11}{12}, \frac{1}{12}), (\frac{25}{27}, \frac{22}{27}, \frac{1}{9}), (\frac{55}{72}, \frac{5}{9}, \frac{5}{24})$
$\frac{5}{2}$	(92)	2	$\frac{1}{2}$	1,2,3,4	$(1, \frac{8}{9}, \frac{1}{9}), (1, \frac{11}{12}, \frac{1}{12}), (1, \frac{22}{27}, \frac{5}{27}), (\frac{65}{72}, \frac{5}{9}, \frac{25}{72})$
$\frac{5}{2}$	(94)	4	$\frac{7}{24}$	1,2,3,4	$(1.0, 0.732, 0.268), (1.0, 0.671, 0.329), (1.0, 0.596, 0.404), (1.0, 0.458, 0.542)$

Table I. Summary of mixed spin states discussed in Sec. VB. For each state, the table lists the spin  $j$ , the equation defining the state, its rank, its purity  $\text{Tr}(\rho^2)$ , and the AC orders of the evaluated measures in the last column. The purity-based total, quantum, and classical contributions  $(\mathcal{A}_t^{T,\mathcal{P}}, \mathcal{A}_t^{Q,\mathcal{P}}, \mathcal{A}_t^{C,\mathcal{P}})$  are given. Decimal entries are numerical convex-roof evaluations. States with  $\mathcal{A}_t^{T,\mathcal{P}} = 1$  are exactly  $t$ -anticoherent.

its original formulation, spin  $t$ -anticoherence is a property of maximal isotropy: a spin state is  $t$ -anticoherent when all spin moments up to order  $t$  are independent of direction, or equivalently when all multipole moments up to rank  $t$  vanish. For mixed states, we recast this condition using the symmetric  $N = 2j$  qubit embedding, where it is equivalently expressed by maximal mixedness of the reduced symmetric  $t$ -qubit state  $\rho_t$ . This reformulation led to an axiomatic separation between *total*  $t$ -anticoherence, which quantifies isotropy independently of its origin, and *quantum*  $t$ -anticoherence, which isolates the genuinely quantum contribution as a resource monotone associated with a chosen total measure. Their difference defines a *classical* contribution, capturing isotropy produced by statistical mixing.

On the constructive side, we introduced broad families of total measures based on normalized distances from  $\rho_t$  to the MMS state, including a Hilbert–Schmidt distance-based measure and a fidelity-based total candidate, as well as simple purity-based and cumulative-multipole measures. The total monotonicity of the fidelity-based candidate under all  $\text{SU}(2)$ -covariant channels remains supported by numerical evidence. We also showed how cumulative multipole functionals fit naturally into the same axiomatic picture, thereby clarifying the relation with earlier tensor-based descriptions of angular structure. For the quantum contribution, we constructed convex-roof extensions from pure-state functionals tied to bipartite entanglement across the  $t | N-t$  split, obtaining explicit purity/linear-entropy-based quantum measures and a fidelity/convex-roof-negativity construction satisfying the quantum-side requirements and the ordering relative to the fidelity-based total candidate. For the constructions where the required ordering is established, the inequality  $\mathcal{A}_t^Q \leq \mathcal{A}_t^T$  ensures a well-defined and non-negative classical part  $\mathcal{A}_t^C = \mathcal{A}_t^T - \mathcal{A}_t^Q$ .

Our examples illustrate that mixed-state anticoherence exhibits qualitatively new behavior absent in the pure-state regime. In particular, mixed states supported on  $t$ -AC subspaces can retain *maximal quantum*  $t$ -anticoherence independently of the mixing weights, showing that perfect isotropy need not be of classical origin. Conversely, when the achievable anticoherence order is

increased at fixed purity, the total isotropy typically becomes more classical: higher-order isotropy is accessible only at sufficiently low purity, and its quantum share generally decreases. We also showed contrasting robustness patterns under particle loss, with HOAP, GHZ, and  $W$  states displaying markedly different decay profiles of the quantum contribution.

A conceptual message of this work is that *isotropy of quantum origin* can itself be viewed as a resource, complementary to the usual resource-theoretic viewpoint in which  $\text{SU}(2)$ -*asymmetry* is the resource. In the asymmetry framework, useful states are those that break rotational symmetry and carry directional information. Here, by contrast, the quantum measure  $\mathcal{A}_t^Q$  isolates the part of isotropy that cannot be reproduced by classical randomization over directions. It therefore identifies states that are direction-insensitive for intrinsically quantum reasons, encoded in genuine multipartite correlations in the symmetric sector. This entanglement-based perspective is already built into our axioms, through the requirements of vanishing on separable symmetric states and monotonicity under LOCC, and is made concrete by the explicit measures introduced here. The resulting distinction is operationally relevant whenever one wishes to separate loss of directional information caused by uncontrolled classical noise from isotropy engineered coherently through entanglement.

Several directions follow naturally. It would be interesting to sharpen the operational role of total, quantum, and classical anticoherence in concrete reference-frame alignment and direction-estimation protocols, and to characterize optimal states under constraints such as purity, rank, or particle loss. On the structural side, a broader classification of  $t$ -AC subspaces and of mixed states saturating the convex-roof constructions would clarify the landscape of extremal isotropic resources. Finally, although our analysis focuses on permutation-symmetric sectors and  $\text{SU}(2)$ , the same strategy should extend to other symmetry groups and multipartite settings, providing a general route to separate intrinsically quantum isotropy from isotropy generated by classical uncertainty.

## ACKNOWLEDGEMENTS

JM and ESE thank Nicolas Cerf for stimulating discussions on this topic. This work is supported by the Quantum Science and Technology - National Science and Technology Major Project (Grant No. 2025ZD0300801) and the National Natural Science Foundation of China (Grant Nos. 92476201). JM and ESE acknowledge the FWO and the F.R.S.-FNRS for their funding as part of the Excellence of Science programme (EOS project 40007526).

## Appendix A: Proofs

We begin this Appendix on the proofs of our propositions by two useful results. A general observation is that the ordering axiom (Q6) follows automatically whenever the chosen total measure is concave.

**Proposition 10.** *Let  $\mathcal{A}_t^T : \mathcal{D}(\mathcal{H}_j) \rightarrow [0, 1]$  be a total  $t$ -anticoherence measure whose restriction to pure states is used to define*

$$\mathcal{A}_t^Q(\rho) = \min_{\{p_i, |\psi_i\rangle\}} \sum_i p_i \mathcal{A}_t^T(|\psi_i\rangle\langle\psi_i|). \quad (\text{A1})$$

If  $\mathcal{A}_t^T$  is concave on  $\mathcal{D}(\mathcal{H}_j)$ , then

$$\mathcal{A}_t^Q(\rho) \leq \mathcal{A}_t^T(\rho) \quad \forall \rho \in \mathcal{D}(\mathcal{H}_j), \quad (\text{A2})$$

i.e., axiom (Q6) holds.

*Proof.* Let  $\rho = \sum_i p_i |\psi_i\rangle\langle\psi_i|$  be any pure-state decomposition. By concavity of  $\mathcal{A}_t^T$ ,

$$\mathcal{A}_t^T(\rho) \geq \sum_i p_i \mathcal{A}_t^T(|\psi_i\rangle\langle\psi_i|). \quad (\text{A3})$$

Since this inequality holds for every decomposition, it also holds for the one minimizing the convex roof, which gives

$$\mathcal{A}_t^T(\rho) \geq \mathcal{A}_t^Q(\rho). \quad (\text{A4})$$

□

We will also need a result derived in [61].

**Theorem 2 ([61]).** *Let  $f : \mathcal{D}(\mathcal{H}_{t/2}) \rightarrow \mathbb{R}$  be concave and invariant under unitary operations. Then the pure-state functional*

$$\mathcal{A}_t^Q(|\psi\rangle) = f(\text{Tr}_{N-t}(|\psi\rangle\langle\psi|)) \quad (\text{A5})$$

is non-increasing on average under LOCC operations across the bipartition  $t | N-t$ . Its convex-roof extension,

$$\mathcal{A}_t^Q(\rho) = \min_{\{p_i, |\psi_i\rangle\}} \sum_i p_i \mathcal{A}_t^Q(|\psi_i\rangle), \quad (\text{A6})$$

is non-increasing under LOCC operations across that bipartition.

## 1. Proof of Prop. 1

*Proof.* First,  $\text{Tr}(\rho_t^2) = 1/(t+1)$  if and only if  $\rho_t$  is maximally mixed, which gives (T1).

Let us now prove (T2). If  $\rho$  is a pure coherent state, then every reduced state  $\rho_t$  is pure, so  $\text{Tr}(\rho_t^2) = 1$  and hence  $\mathcal{A}_t^{T,\mathcal{P}}(\rho) = 0$ . Conversely, if  $\mathcal{A}_t^{T,\mathcal{P}}(\rho) = 0$ , then  $\text{Tr}(\rho_t^2) = 1$ , so  $\rho_t$  is pure. Since  $\rho_t$  is obtained by tracing out part of the symmetric  $N$ -qubit state  $\rho_S$ , the purity of  $\rho_t$  implies that  $\rho_S$  is product across the bipartition  $t | N-t$ . Because  $\rho_S$  is supported on the fully symmetric subspace, separability across this bipartition is equivalent to full separability [50]; hence  $\rho_S$  is a convex mixture of symmetric product states. The fact that  $\rho_t$  is pure then forces this mixture to contain only one product component, so  $\rho_S = (|\mathbf{n}\rangle\langle\mathbf{n}|)^{\otimes N}$ , i.e.  $\rho$  is a pure spin-coherent state. This proves (T2).

The SU(2) invariance (T3) is inherited from the invariance of  $\text{Tr}(\rho_t^2)$  under global rotations, and normalization to  $[0, 1]$  is ensured by the prefactor  $(t+1)/t$ .

We now prove monotonicity under SU(2)-covariant noise (T4). Let  $\Phi$  be an SU(2)-covariant channel on  $\mathcal{H}_j$ . By covariance, the multipole coefficients transform as  $\rho_{LM} \mapsto f_L \rho_{LM}$  with  $|f_L| \leq 1$ . For compactness, write

$$c_{N,t,L} = \frac{t!}{N!} \sqrt{\frac{(N-L)!(N+L+1)!}{(t-L)!(t+L+1)!}}, \quad (\text{A7})$$

so that Eq. (6) reads

$$\rho_t = \frac{\mathbb{1}_{t+1}}{t+1} + \sum_{L=1}^t \sum_{M=-L}^L c_{N,t,L} \rho_{LM} T_{LM}^{(t)}. \quad (\text{A8})$$

Using the Hilbert–Schmidt normalization of the tensors  $T_{LM}^{(t)}$ , we obtain

$$\begin{aligned} \text{Tr}([\Phi(\rho)]_t^2) &= \frac{1}{t+1} + \sum_{L=1}^t c_{N,t,L}^2 f_L^2 \sum_{M=-L}^L |\rho_{LM}|^2 \\ &\leq \frac{1}{t+1} + \sum_{L=1}^t c_{N,t,L}^2 \sum_{M=-L}^L |\rho_{LM}|^2 \\ &= \text{Tr}(\rho_t^2). \end{aligned} \quad (\text{A9})$$

Hence  $\mathcal{A}_t^{T,\mathcal{P}}(\Phi(\rho)) \geq \mathcal{A}_t^{T,\mathcal{P}}(\rho)$ , proving (T4). □

## 2. Proof of Prop. 2

*Proof.* Axioms (T1)–(T3) follow from the general distance-based construction. We now prove (T4) as in Prop. 1. Using the notation (A7) together with the ex-

pansion of  $\rho_t$  in Eq. (6), we have

$$\begin{aligned} \|(\Phi(\rho))_t - \rho_0^{(t)}\|_2^2 &= \sum_{L=1}^t \sum_{M=-L}^L c_{N,t,L}^2 |f_L|^2 |\rho_{LM}|^2 \\ &\leq \sum_{L=1}^t \sum_{M=-L}^L c_{N,t,L}^2 |\rho_{LM}|^2 \\ &= \|\rho_t - \rho_0^{(t)}\|_2^2, \end{aligned} \quad (\text{A10})$$

because  $|f_L| \leq 1$  for all  $L$ . Hence the Hilbert–Schmidt measure

$$\mathcal{A}_t^{T,\text{HS}}(\rho) = 1 - \frac{\|\rho_t - \rho_0^{(t)}\|_2}{K_t^{\text{HS}}} \quad (\text{A11})$$

also satisfies axiom (T4).  $\square$

### 3. Proof of Prop. 3

*Proof.* From the Schmidt decomposition, it can be seen that the reduced state of  $|\psi\rangle$  on  $A$  is given by

$$\rho_A = \sum_{i=1}^{d_A} \alpha_i^2 |\phi_A^{(i)}\rangle \langle \phi_A^{(i)}|, \quad (\text{A12})$$

So, the eigenvalues  $\lambda_i$  of  $\rho_A$  are related to the Schmidt coefficients  $\alpha_i$ , that is,  $\lambda_i = \alpha_i^2$ . For pure states  $\rho = |\psi\rangle\langle\psi|$ , the fidelity between  $\rho_A$  and the MMS verifies

$$F(\rho_A, \rho_0) = \frac{1}{d_A} (\text{Tr} \sqrt{\rho_A})^2 = \frac{1}{d_A} \left( \sum_{i=1}^{d_A} \sqrt{\lambda_i} \right)^2. \quad (\text{A13})$$

The eigenvalues of the reduced state  $\rho_A$  verify

$$\left( \sum_{i=1}^{d_A} \sqrt{\lambda_i} \right)^2 = \underbrace{\sum_{i=1}^{d_A} \lambda_i}_{=1} + 2 \sum_{i>j=1}^{d_A} \sqrt{\lambda_i \lambda_j} \quad (\text{A14})$$

and from (29), we see that [51]

$$\left( \sum_{i=1}^{d_A} \sqrt{\lambda_i} \right)^2 = 1 + 2\mathcal{N}_A(|\psi\rangle). \quad (\text{A15})$$

Injecting (A15) in (A13), we obtain our result (30).  $\square$

### 4. Proof of Prop. 4

*Proof.* Pure-state consistency (Q2) and SU(2) invariance (Q3) are immediate from the definition and the rotational covariance of the reduced state. Convexity (Q4) follows directly from the convex-roof construction. Axiom (Q5) follows from Theorem 2 since the function  $f(\rho) = 1 - \text{Tr}(\rho^2)$  is concave and invariant under unitaries due to

the properties of the purity. Axiom (Q1) follows because fully separable symmetric states admit decompositions into coherent states, and  $\mathcal{A}_t^P$  vanishes on pure coherent states.

To prove (Q6), it is enough to note that the total purity-based measure  $\mathcal{A}_t^{T,P}(\rho) = \frac{t+1}{t}(1 - \text{Tr}(\rho_t^2))$  is concave (equivalently,  $-\text{Tr}(\rho_t^2)$  is concave because  $\text{Tr}(\rho_t^2)$  is convex and  $\rho \mapsto \rho_t$  is linear). Therefore the ordering follows directly from the general convex-roof ordering Proposition 10.  $\square$

### 5. Proof of Prop. 5

*Proof.* For pure states  $|\psi\rangle$ , the reduced density matrices across the bipartitions  $t|N-t$  and  $(N-t)|t$  have identical nonzero spectra, which implies  $\text{Tr}(\rho_t^2) = \text{Tr}(\rho_{N-t}^2)$  and therefore

$$\mathcal{A}_t^P(|\psi\rangle) = c_t \mathcal{A}_{N-t}^P(|\psi\rangle), \quad c_t = \frac{(t+1)(N-t)}{t(N+1-t)}. \quad (\text{A16})$$

Let  $\rho = \sum_i p_i |\psi_i\rangle\langle\psi_i|$  be an arbitrary pure-state decomposition. Using the above relation term by term yields

$$\sum_i p_i \mathcal{A}_t^P(|\psi_i\rangle) = c_t \sum_i p_i \mathcal{A}_{N-t}^P(|\psi_i\rangle). \quad (\text{A17})$$

Since this equality holds for every decomposition, it also holds for the minimizing decompositions defining the convex-roof extensions, giving

$$\mathcal{A}_t^{Q,P}(\rho) = c_t \mathcal{A}_{N-t}^{Q,P}(\rho), \quad (\text{A18})$$

which proves the claim.  $\square$

### 6. Proof of Prop. 6

*Proof.* Axioms (Q2) and (Q4) follow directly from the convex-roof construction, while axiom (Q3) follows from the SU(2) invariance of the pure-state functional. Axiom (Q5) follows by assumption, since  $\mathcal{A}_t^d(|\psi\rangle)$  is an entanglement monotone across the bipartition  $t|N-t$  and convex roofs of pure-state entanglement monotones are LOCC monotones. Axiom (Q1) follows because the pure-state functional vanishes on coherent states, and fully separable symmetric states admit decompositions into coherent states. Finally, if  $\mathcal{A}_t^{T,d}$  is concave, axiom (Q6) follows from Proposition 10.  $\square$

### 7. Proof of Prop. 7

*Proof.* We first recall the definition of the total fidelity-based measure:

$$\mathcal{A}_t^{T,F}(\rho) = \frac{(\text{Tr}(\sqrt{\rho_t}))^2 - 1}{t} = \frac{(t+1)F(\rho_t, \rho_0^{(t)}) - 1}{t}. \quad (\text{A19})$$

As discussed in Sec. III A 3, this quantity satisfies axioms (T1)–(T3). Indeed, (T1) follows from  $F(\rho_t, \rho_0^{(t)}) = 1$  iff  $\rho_t = \rho_0^{(t)}$ , while (T2) follows from the fact that  $F(\rho_t, \rho_0^{(t)}) = 1/(t+1)$  iff  $\rho_t$  is pure, which in the symmetric sector forces the global state to be a pure spin-coherent state. Axiom (T3) follows from unitary invariance of fidelity.

We now prove the quantum axioms for

$$\mathcal{A}_t^{Q,F}(\rho) = \frac{2}{t} \mathcal{N}_t^{\text{CR}}(\rho). \quad (\text{A20})$$

Axiom (Q1) holds because every fully separable symmetric state admits a decomposition into coherent states, and the negativity vanishes on each coherent pure state. Axiom (Q3) follows because global rotations act by local unitaries with respect to the bipartition  $t|N-t$ , and therefore do not change the negativity. Convexity (Q4) follows directly from the convex-roof construction, and monotonicity under LOCC operations (Q5) follows from the corresponding property of the convex-roof negativity [52].

It remains to verify pure-state consistency (Q2) and the ordering axiom (Q6). For pure states, Proposition 3 gives

$$F(\rho_t, \rho_0^{(t)}) = \frac{1 + 2\mathcal{N}_t(|\psi\rangle)}{t+1}. \quad (\text{A21})$$

Therefore,

$$\begin{aligned} \mathcal{A}_t^{T,F}(|\psi\rangle) &= \frac{(t+1)F(\rho_t, \rho_0^{(t)}) - 1}{t} \\ &= \frac{2}{t} \mathcal{N}_t(|\psi\rangle) = \mathcal{A}_t^{Q,F}(|\psi\rangle), \end{aligned} \quad (\text{A22})$$

which proves (Q2).

For (Q6), let  $\rho = \sum_i p_i |\psi_i\rangle\langle\psi_i|$  be an arbitrary pure-state decomposition and define  $\sigma_i = \text{Tr}_{N-t}(|\psi_i\rangle\langle\psi_i|)$ , so that  $\rho_t = \sum_i p_i \sigma_i$ . We use the superadditivity of the Schatten 1/2-quasinorm [62],

$$\|A+B\|_{1/2} \geq \|A\|_{1/2} + \|B\|_{1/2}, \quad \|X\|_{1/2} = (\text{Tr}(\sqrt{X}))^2, \quad (\text{A23})$$

for positive semidefinite operators. By positive homogeneity,

$$\begin{aligned} (\text{Tr}(\sqrt{\rho_t}))^2 &= \left\| \sum_i p_i \sigma_i \right\|_{1/2} \geq \sum_i \|p_i \sigma_i\|_{1/2} \\ &= \sum_i p_i (\text{Tr}(\sqrt{\sigma_i}))^2. \end{aligned} \quad (\text{A24})$$

For each pure state  $|\psi_i\rangle$ ,

$$(\text{Tr}(\sqrt{\sigma_i}))^2 = 1 + 2\mathcal{N}_t(|\psi_i\rangle). \quad (\text{A25})$$

Hence

$$(\text{Tr}(\sqrt{\rho_t}))^2 \geq 1 + 2 \sum_i p_i \mathcal{N}_t(|\psi_i\rangle). \quad (\text{A26})$$

Since this is true for every pure-state decomposition, it is true in particular for an optimal decomposition of the convex roof. Thus

$$(\text{Tr}(\sqrt{\rho_t}))^2 \geq 1 + 2\mathcal{N}_t^{\text{CR}}(\rho), \quad (\text{A27})$$

and consequently

$$\mathcal{A}_t^{T,F}(\rho) = \frac{(\text{Tr}(\sqrt{\rho_t}))^2 - 1}{t} \geq \frac{2}{t} \mathcal{N}_t^{\text{CR}}(\rho) = \mathcal{A}_t^{Q,F}(\rho). \quad (\text{A28})$$

This proves (Q6).  $\square$

## 8. Proof of Prop. 8

*Proof.* We first show that  $\mathcal{A}_t^{T,\text{cm}}(\rho)$  is indeed a function taking values in  $[0, 1]$ , which is equivalent to proving that  $0 \leq C_{\leq t}(\rho) \leq C_{\leq t}(\rho_{\text{coh}})$ . Since it is a sum of positive quantities, it is immediate to verify that  $C_{\leq t}(\rho) \geq 0$ . The upper bound is proved in the following lemma:

**Lemma 2.** *For every spin- $j$  density matrix  $\rho$  and every  $t = 1, \dots, 2j-1$ ,*

$$C_{\leq t}(\rho) \leq C_{\leq t}(\rho_{\text{coh}}), \quad (\text{A29})$$

where  $\rho_{\text{coh}}$  is any spin-coherent state.

*Proof.* For pure states, the bound follows from the extremality of SU(2) coherent states for the cumulative multipole distribution: coherent states maximize  $C_{\leq t}$  at every order  $t$  [3]. For mixed states, write  $\rho = \sum_i p_i |\psi_i\rangle\langle\psi_i|$ . Since  $C_{\leq t}$  is the squared Hilbert–Schmidt norm of the projection of  $\rho$  onto the subspace spanned by the tensor operators  $T_{LM}$  with  $1 \leq L \leq t$ , it is convex. Hence

$$C_{\leq t}(\rho) \leq \sum_i p_i C_{\leq t}(|\psi_i\rangle\langle\psi_i|) \leq C_{\leq t}(\rho_{\text{coh}}). \quad (\text{A30})$$

$\square$

We now verify the defining properties of  $\mathcal{A}_t^{T,\text{cm}}(\rho)$ . Axiom (T1) follows directly from the affine normalization in Eq. (42): by definition,  $C_{\leq t}(\rho) = 0$  if and only if all multipoles up to rank  $t$  vanish, i.e. if and only if  $\rho$  is  $t$ -AC. For axiom (T2),  $\mathcal{A}_t^{T,\text{cm}}(\rho) = 0$  if and only if  $\rho$  is a pure coherent state, using the coherent-state extremality in Lemma 2 together with the uniqueness of the pure-state maximizers. Axiom (T3) holds because under a global rotation the coefficients  $\rho_{LM}$  transform unitarily within each fixed  $L$ , so each  $a_L(\rho) \equiv \sum_{M=-L}^L |\rho_{LM}|^2$  is invariant, hence so is  $C_{\leq t}(\rho)$ .

It remains to verify axiom (T4). Let  $\Phi$  be an SU(2)-covariant channel on  $\mathcal{H}_j$ . By the standard structure theorem for covariant channels on a fixed spin irrep (see Sec. II B around Eq. (10)),  $\Phi$  acts diagonally on irreducible tensor operators:

$$\Phi(T_{LM}) = f_L T_{LM}, \quad (\text{A31})$$

with  $f_L$  independent of  $M$  and satisfying  $|f_L| \leq 1$ . Therefore, if

$$\rho = \frac{\mathbb{1}}{2j+1} + \sum_{L=1}^{2j} \sum_{M=-L}^L \rho_{LM} T_{LM}, \quad (\text{A32})$$

then for  $\rho' = \Phi(\rho)$  one has  $\rho'_{LM} = f_L \rho_{LM}$ , and thus

$$\sum_{M=-L}^L |\rho'_{LM}|^2 = |f_L|^2 \sum_{M=-L}^L |\rho_{LM}|^2 \leq \sum_{M=-L}^L |\rho_{LM}|^2. \quad (\text{A33})$$

Summing over  $L = 1, \dots, t$  gives

$$C_{\leq t}(\Phi(\rho)) \leq C_{\leq t}(\rho). \quad (\text{A34})$$

Since  $\mathcal{A}_t^{T,\text{cm}}$  is an affine decreasing function of  $C_{\leq t}$ , it

follows that

$$\mathcal{A}_t^{T,\text{cm}}(\Phi(\rho)) \geq \mathcal{A}_t^{T,\text{cm}}(\rho), \quad (\text{A35})$$

which is axiom (T4).  $\square$

## 9. Proof of Prop. 9

*Proof.* For  $t = 1$ ,  $C_{\leq 1}(\rho)$  is affine in the one-body reduced purity  $r_1 = \text{Tr}(\rho_1^2)$  (equivalently, in  $|\langle \mathbf{J} \rangle|^2$ ) by the standard purity–multipole relations for symmetric states. Therefore, after normalization to  $[0, 1]$  with coherent states mapped to 0 and 1-AC pure states to 1, the pure-state functionals  $\mathcal{A}_1^{T,\text{cm}}(|\psi\rangle)$  and  $\mathcal{A}_1^{\mathcal{P}}(|\psi\rangle)$  coincide.

Taking convex roofs of the same pure-state functional gives

$$\mathcal{A}_1^{Q,\text{cm}}(\rho) = \mathcal{A}_1^{Q,\mathcal{P}}(\rho). \quad (\text{A36})$$

Since  $\mathcal{A}_1^{Q,\mathcal{P}}$  satisfies axioms (Q1)–(Q6) by Proposition 4, the same is true for  $\mathcal{A}_1^{Q,\text{cm}}$ , in particular (Q5).  $\square$

- 
- [1] J. Zimba, *Electronic Journal of Theoretical Physics* **3**, 143 (2006).
- [2] M. Rudziński, A. Burchardt, and K. Życzkowski, *Quantum* **8**, 1234 (2024).
- [3] G. Björk, A. B. Klimov, P. de la Hoz, M. Grassl, G. Leuchs, and L. L. Sánchez-Soto, *Phys. Rev. A* **92**, 031801(R) (2015).
- [4] J. Crann, R. Pereira, and D. W. Kribs, *J. Phys. A: Math. Theor.* **43**, 255307 (2010).
- [5] D. Baguette, F. Damanet, O. Giraud, and J. Martin, *Phys. Rev. A* **92**, 052333 (2015).
- [6] E. Serrano-Ensástiga and D. Braun, *Phys. Rev. A* **101**, 022332 (2020).
- [7] D. Baguette, T. Bastin, and J. Martin, *Phys. Rev. A* **90**, 032314 (2014).
- [8] P. Kolenderski and R. Demkowicz-Dobrzanski, *Phys. Rev. A* **78**, 052333 (2008).
- [9] C. Chryssomalakos and H. Hernández-Coronado, *Phys. Rev. A* **95**, 052125 (2017).
- [10] A. Z. Goldberg and D. F. V. James, *Phys. Rev. A* **98**, 032113 (2018).
- [11] J. Martin, S. Weigert, and O. Giraud, *Quantum* **4**, 285 (2020).
- [12] H. Ferretti, Y. B. Yilmaz, K. Bonsma-Fisher, A. Z. Goldberg, N. Lupu-Gladstein, A. O. T. Pang, L. A. Rozema, and A. M. Steinberg, *Optica Quantum* **2**, 91 (2024).
- [13] J. M. Robbins and M. V. Berry, *Journal of Physics A: Mathematical and General* **27**, L435 (1994).
- [14] P. Aguilar, C. Chryssomalakos, E. Guzmán-González, L. Hanotel, and E. Serrano-Ensástiga, *Journal of Physics A: Mathematical and Theoretical* **53**, 065301 (2020).
- [15] C. Chryssomalakos, L. Hanotel, E. Guzmán-González, and E. Serrano-Ensástiga, *Mod. Phys. Lett. A* **37**, 2250184 (2022).
- [16] J. R. Hervas, A. Z. Goldberg, A. S. Sanz, Z. Hradil, J. Řeháček, and L. L. Sánchez-Soto, *Phys. Rev. Lett.* **134**, 010804 (2025).
- [17] S.-H. Chiew and M. Gessner, *Phys. Rev. Res.* **4**, 013076 (2022).
- [18] S. Massar and S. Popescu, *Phys. Rev. Lett.* **74**, 1259 (1995).
- [19] N. Gisin and S. Popescu, *Phys. Rev. Lett.* **83**, 432 (1999).
- [20] A. Peres and P. F. Scudo, *Phys. Rev. Lett.* **86**, 4160 (2001).
- [21] A. Peres and P. F. Scudo, *Phys. Rev. Lett.* **87**, 167901 (2002).
- [22] A. Peres and P. Scudo, *Journal of Modern Optics* **49**, 1235 (2002).
- [23] D. Collins and S. Popescu, arXiv preprint quant-ph/0401096 (2004), arXiv:quant-ph/0401096.
- [24] E. Chitambar and G. Gour, *Rev. Mod. Phys.* **91**, 025001 (2019).
- [25] S. D. Bartlett, T. Rudolph, and R. W. Spekkens, *Rev. Mod. Phys.* **79**, 555 (2007).
- [26] G. Gour and R. W. Spekkens, *New J. Phys.* **10**, 033023 (2008).
- [27] G. Gour, I. Marvian, and R. W. Spekkens, *Phys. Rev. A* **80**, 012307 (2009).
- [28] E. Chitambar and G. Gour, *Rev. Mod. Phys.* **91**, 025001 (2019).
- [29] E. Serrano-Ensástiga, C. Chryssomalakos, and J. Martin, *Phys. Rev. A* **111**, 022435 (2025).
- [30] F. Bouchard, P. de la Hoz, G. Björk, R. W. Boyd, M. Grassl, Z. Hradil, E. Karimi, A. B. Klimov, G. Leuchs, J. Řeháček, and L. L. Sánchez-Soto, *Optica* **4**, 1429 (2017).
- [31] J. Denis, C. Read, and J. Martin, *SciPost Phys. Core* **9**, 001 (2026).

- [32] A. Z. Goldberg, J. R. Hervas, A. S. Sanz, A. B. Klimov, J. Řeháček, Z. Hradil, M. Hiekkamäki, M. Eriksson, R. Fickler, G. Leuchs, and L. L. Sánchez-Soto, *Quantum Science and Technology* **10**, 015053 (2024).
- [33] J. Bringewatt, L. Zaporski, M. Radzihovsky, J. Albert, A. V. Gorshkov, V. Vuletic, and G. Bentsen, *Butterfly echo protocol for axis-agnostic heisenberg-limited metrology* (2026), [arXiv:2602.23332 \[quant-ph\]](https://arxiv.org/abs/2602.23332).
- [34] D. Baguette and J. Martin, *Phys. Rev. A* **96**, 032304 (2017).
- [35] E. Majorana, *Il Nuovo Cimento (1924-1942)* **9**, 43 (1932).
- [36] M. Aulbach, D. Markham, and M. Muraio, *New J. Phys.* **12**, 073025 (2010).
- [37] M. Aulbach, *Int. J. Quantum Inf.* **10**, 1230004 (2012).
- [38] P. de la Hoz, A. B. Klimov, G. Björk, Y.-H. Kim, C. Müller, C. Marquardt, G. Leuchs, and L. L. Sánchez-Soto, *Phys. Rev. A* **88**, 063803 (2013).
- [39] L. L. Sánchez-Soto, A. B. Klimov, P. de la Hoz, and G. Leuchs, *J. Phys. B: At. Mol. Opt. Phys.* **46**, 104011 (2013).
- [40] D. A. Varshalovich, A. N. Moskalev, and V. K. Khersonskii, *Quantum Theory of Angular Momentum* (World Scientific, 1988).
- [41] J. Denis and J. Martin, *Phys. Rev. Res.* **4**, 013178 (2022).
- [42] O. Giraud, D. Braun, D. Baguette, T. Bastin, and J. Martin, *Phys. Rev. Lett.* **114**, 080401 (2015).
- [43] I. Marvian and R. W. Spekkens, *Nat. Commun.* **5**, 3821 (2014).
- [44] I. Marvian and R. W. Spekkens, *Phys. Rev. A* **90**, 014102 (2014).
- [45] A. S. Holevo, *Remarks on the classical capacity of quantum channel* (2002), [arXiv:quant-ph/0212025](https://arxiv.org/abs/quant-ph/0212025).
- [46] C. Müller, Diffusive spin transport, in *Entanglement and Decoherence: Foundations and Modern Trends*, edited by A. Buchleitner, C. Viviescas, and M. Tiersch (Springer Berlin Heidelberg, Berlin, Heidelberg, 2009) pp. 277–314.
- [47] Á. Rivas and A. Luis, *Phys. Rev. A* **88**, 052120 (2013).
- [48] E. Chang, J. Kim, H. Kwak, H. H. Lee, and S.-G. Youn, *Reviews in Mathematical Physics* **34**, 2250021 (2022).
- [49] T. Aschieri, B. Ruba, and J. P. Solovej, *Communications in Mathematical Physics* **405**, 298 (2024).
- [50] T. Ichikawa, T. Sasaki, I. Tsutsui, and N. Yonezawa, *Physical Review A* **78**, 052105 (2008).
- [51] G. Vidal and R. F. Werner, *Phys. Rev. A* **65**, 032314 (2002).
- [52] S. Lee, D. P. Chi, S. D. Oh, and J. Kim, *Phys. Rev. A* **68**, 062304 (2003).
- [53] A. Z. Goldberg, A. B. Klimov, H. deGuise, G. Leuchs, G. S. Agarwal, and L. L. Sánchez-Soto, *Optics Letters* **47**, 477 (2022).
- [54] A. Z. Goldberg, P. de la Hoz, G. Björk, A. B. Klimov, M. Grassl, G. Leuchs, and L. L. Sánchez-Soto, *Advances in Optics and Photonics* **13**, 1 (2021).
- [55] M. A. Nielsen, *Phys. Rev. Lett.* **83**, 436 (1999).
- [56] R. Pereira and C. Paul-Paddock, *J. Math. Phys.* **58**, 062107 (2017).
- [57] J. A. Gross, *Phys. Rev. Lett.* **127**, 010504 (2021).
- [58] S. Lim, J. Liu, and A. Ardavan, *Phys. Rev. A* **108**, 062403 (2023).
- [59] X. Zhu, C. Zhang, Z. An, and B. Zeng, *npj Quantum Information* **11**, 56 (2025).
- [60] W. Kłobus, A. Burchardt, A. Kołodziejcki, M. Pandit, T. Vértesi, K. Życzkowski, and W. Laskowski, *Phys. Rev. A* **100**, 032112 (2019).
- [61] G. Vidal, *Journal of Modern Optics* **47**, 355 (2000).
- [62] J.-C. Bourin and F. Hiai, *International Journal of Mathematics* **22**, 1121 (2011).